

Quantum feedback control of a two-atom network closed by a semi-infinite waveguide

Haijin Ding^a, Guofeng Zhang^{a,b,*}, Mu-Tian Cheng^c, Guoqing Cai^c

^aDepartment of Applied Mathematics, The Hong Kong Polytechnic University, Hung Hom, Kowloon, Hong Kong

^bThe Hong Kong Polytechnic University Shenzhen Research Institute, Shenzhen, 518057, China

^cSchool of Electrical and Information Engineering, Anhui University of Technology, Maanshan, 243003, China

Abstract

The purpose of this paper is to study the delay-dependent coherent feedback dynamics by focusing on one typical realization, i.e., a two-atom quantum network whose feedback loop is closed by a semi-infinite waveguide. In this set-up, an initially excited two-level atom can emit a photon into the waveguide, where the propagating photon can be reflected by the terminal mirror of the waveguide or absorbed by the other atom, thus constructing various coherent feedback loops. We show that there can be two-photon, one-photon or zero-photon states in the waveguide, which can be controlled by the feedback loop length and the coupling strengths between the atoms and waveguide. The photonic states in the waveguide are analyzed in both the frequency domain and the spatial domain, and the transient process of photon emissions is better understood based on a comprehensive analysis using both domains. Interestingly, we clarify that this quantum coherent feedback network can be mathematically modeled as a linear control system with multiple delays, which are determined by the distances between atoms and the terminal mirror of the semi-infinite waveguide. Therefore, based on time-delayed linear control system theory, the influence of delays on the stability of the quantum state evolution and the steady-state atomic and photonic states is investigated, for both small and large delays.

Keywords: Quantum coherent feedback control; delayed linear systems; waveguide QED; atom-waveguide interactions.

Contents

1	Introduction	2
2	Feedback control for two atoms coupled with a waveguide in the frequency domain	4
2.1	Control the photon number in the waveguide by means of delay and chiral couplings	8
2.2	The relationship between delay and the coherent feedback network model	12

*Corresponding author

Email addresses: dhj17@tsinghua.org.cn (Haijin Ding), guofeng.zhang@polyu.edu.hk (Guofeng Zhang), mtcheng@ahut.edu.cn (Mu-Tian Cheng), cgq268052@163.com (Guoqing Cai)

2.2.1	Quasi-polynomial model	12
2.2.2	Master equation representation	14
2.3	Atomic dynamics and photon emission analysis	14
3	Feedback control in the spatial domain	16
3.1	One atom coupled with the waveguide	16
3.1.1	The influence of the feedback loop length on stability	19
3.2	The two-atoms dynamics in the spatial domain	21
3.3	Spontaneous emission rate in the spatial domain	22
3.4	Non-exponentially stable dynamics induced by large coherent feedback delays	23
3.5	Comparison with cavity-QED system	24
4	Conclusion	25
Appendix A	Derivations of Eqs. (9,10,11)	26
Appendix B	Derivation of the interaction Hamiltonian in the spatial domain	29
Appendix B.1	The Hamiltonian of the mirror	30
Appendix C	One-atom model in the spatial domain	32
Appendix D	Two-atom model with one excitation in the spatial domain	34

1. Introduction

Quantum feedback control has found a variety of applications in quantum information processing (QIP) and quantum engineering (Zhang et al., 2017). According to whether the quantum state is measured, quantum feedback control can be divided into two categories: measurement feedback control where the feedback control law is designed based on the measurement results of the quantum state (Cardona et al., 2020; Kashima and Yamamoto, 2009; Yamamoto, 2014) and coherent feedback control realized by coherent interactions among various quantum components in a quantum network (Zhang and James, 2010; Zhang, 2020; Zhang and Dong, 2022; Tan et al., 2011). One of the advantages of quantum coherent feedback control is that the evolution of quantum states are not influenced by the noise induced by measuring quantum states.

Among various quantum coherent feedback architectures, one of the most efficient methods is to construct coherent feedback channels using waveguides. In waveguide quantum electro-dynamical (waveguide QED) systems, different components such as atoms (Zhang and Pan, 2020; Zhang et al., 2020) or cavities (Német et al., 2019; Crowder et al., 2020) can be coupled with a waveguide, and photons propagating in the waveguide can realize long-range interactions among atoms or cavities (Simon, 2017; Northup and Blatt, 2014; Monroe, 2002; Flamini et al., 2018). The

quantum network that connects different quantum agents or constructs feedback channels with propagating photons has been experimentally realized in many platforms such as neutral atoms (Hijlkema et al., 2007; Kuhn et al., 2002), superconducting circuits (Houck et al., 2007; Peng et al., 2016), trapped ions (Keller et al., 2004; Barros et al., 2009; Almendros et al., 2009), and quantum dots (Michler et al., 2000; Zwiller et al., 2001).

Similar to control with delays in classical multi-agent networks (Tao et al., 2022; La and Ranjan, 2007; Li and Song, 2016), coherent feedback control based on photons propagating in a waveguide can be regarded as a networked control system with single (Német et al., 2019; Ding and Zhang, 2023) or multiple delays (Zhang et al., 2020; Huo and Li, 2020; Guimond et al., 2017; Pichler and Zoller, 2016). Mechanisms for the occurrence of delays in quantum coherent feedback control can be different for varied architecture designs. For example, in a waveguide QED system where atoms or cavities are coupled with an infinite waveguide (Zhang and Pan, 2020; Laakso and Pletyukhov, 2014; Mirza and Schotland, 2016; Gonzalez-Ballesteros et al., 2015; Dinc, 2020; Cheng et al., 2017; Sinha et al., 2020; Pichler and Zoller, 2016; Regidor et al., 2021; Zheng and Baranger, 2013), the feedback dynamics is only influenced by the transmission delays of photons among atoms or cavities. On the other hand, when the quantum nodes (e.g., atoms or cavities) are coupled to a semi-infinite waveguide (Zhang et al., 2020; Pichler and Zoller, 2016; Regidor et al., 2021; Kockum et al., 2018), the traveling photons can be reflected by the terminal mirror of the waveguide, and therefore the re-interactions between quantum nodes and the reflected photons can construct an additional feedback channel, which is influenced by the distance between the quantum nodes and the terminal mirror of the waveguide.

Recently, the quantum dynamics of atoms coupled with a semi-infinite waveguide has been studied in several scenarios, such as the single-atom circumstance demonstrating controllable emission of single photons (Pichler and Zoller, 2016), the two-atom scheme with one excitation creating entangled states (Zhang et al., 2020), the matrix-product state with multi atoms (Regidor et al., 2021) and the non-Markovian dynamics of giant atoms (Kockum et al., 2018). Depending on whether the coupling strengths between the quantum node (e.g., an atom or a cavity) and the directional photonic field are identical or not, the interaction between the quantum node and the waveguide can be categorized to be nonchiral or chiral (Lodahl et al., 2017), which can be implemented via the waveguide material design and adding external control fields (Mariotte and Engheta, 1993; Busse et al., 1999; Söllner et al., 2015).

Different from classical feedback control and quantum coherent feedback control with cavity quantum electrodynamical (cavity QED) systems (Lang et al., 1973), a waveguide can provide a feedback channel of much larger spatial distribution compared with the size of the quantum nodes, thus inducing much more interesting non-Markovian delayed dynamics. For example, the large spatial distribution of waveguide modes enables the waveguide to couple with the quantum node by means of a series of continuous modes (Német et al., 2019; Crowder et al., 2020), and this can be equivalently modeled in the spatial domain (Shen and Fan, 2009; Bradford and Shen, 2013; Zheng and Baranger, 2013; Yan et al., 2011; Zhou et al., 2017; Hu et al., 2018). In the spatial domain analysis, photons are characterized by their spatial distributions in the waveguide, and the photons emitted by the atoms propagate in the format of wave packets. Based on this, the evolution of the photonic state in the waveguide has been studied in terms of spatial distribution of photonic wave packet in the single-photon and the multi-photon circumstances (Chen et al.,

2017; Bradford and Shen, 2015; Cheng et al., 2017). Clearly, the most desirable way to investigate the coherent feedback dynamics of atoms chirally coupled with a waveguide is a comprehensive analysis according to both the frequency domain and spatial domain modeling.

In summary, for the coherent feedback dynamics with multiple delays realized in waveguide QED systems, mathematical complexity increases with the number of excitations in the quantum network. To our best knowledge, such coherent feedback dynamics with multiple excitations, especially how the dynamics is influenced by multiple delays, has not been systematically investigated from the perspective of control theory. One representative example of such systems is the architecture as shown in Fig. 1, where two two-level atoms are coupled with a semi-infinite waveguide and the network can have at most two excitations. In this set-up, the evolution of the quantum states is simultaneously influenced by the feedback interactions between two atoms as in (Zhang and Pan, 2020), the feedback dynamics induced by the mirror as in (Tufarelli et al., 2013; Bradford and Shen, 2013), and the chiral interactions between the two atoms and the semi-infinite waveguide as in (Zhang et al., 2020). As a result, the photonic states in this system can be controlled by engineering the distance between two atoms, the atom locations relative to the terminal mirror of the semi-infinite waveguide, and the chiral coupling strengths between atoms and the waveguide. By analyzing the dynamics of this coherent feedback network in both the frequency and the spatial domains from the perspective of linear control systems with multiple delays, we show that the steady atomic and photonic states can be different depending on the small or large delays in the coherent feedback network as well as the chiral or nonchiral couplings between the atoms and waveguide.

The rest of the paper is organized as follows. Section 2 analyzes in the frequency domain the coherent feedback dynamics where a semi-infinite waveguide is coupled with two excited two-level atoms, especially the problem how the chiral couplings and delays caused by the locations of atoms influence the performance of the coherent feedback network. Section 3 presents the analysis in the spatial domain and demonstrates how the single-photon wave packet propagates in the two-atom network mediated by a waveguide. Section 4 concludes this paper.

Notation. The reduced Planck constant \hbar , the velocity of the light field c and the group velocity of the propagating photonic wave packets v_g are set to 1 in this paper.

2. Feedback control for two atoms coupled with a waveguide in the frequency domain

As shown in Fig.1, two atoms (or atomlike objects) with the same resonant frequency ω_a are coupled to a semi-infinite waveguide. The distance between the atoms is $L = z_2 - z_1$, where z_j is the location of the j th atom, $j = 1, 2$. The coupling strength between the j th atom with the left-propagating field in the waveguide is γ_{jL} , and that with the right propagating field is γ_{jR} , where γ_{jL} and γ_{jR} are real constant numbers. For the atom at z_1 , the emitted field in the left-propagating direction can be reflected by the mirror at $z = 0$ and then propagates along the right direction to re-interact with the atom, whereas the emitted field in the right-propagating direction excites the atom at z_2 . For the atom at z_2 , the emitted field in the left-propagating direction interacts with the atom at z_1 , while the emitted field in

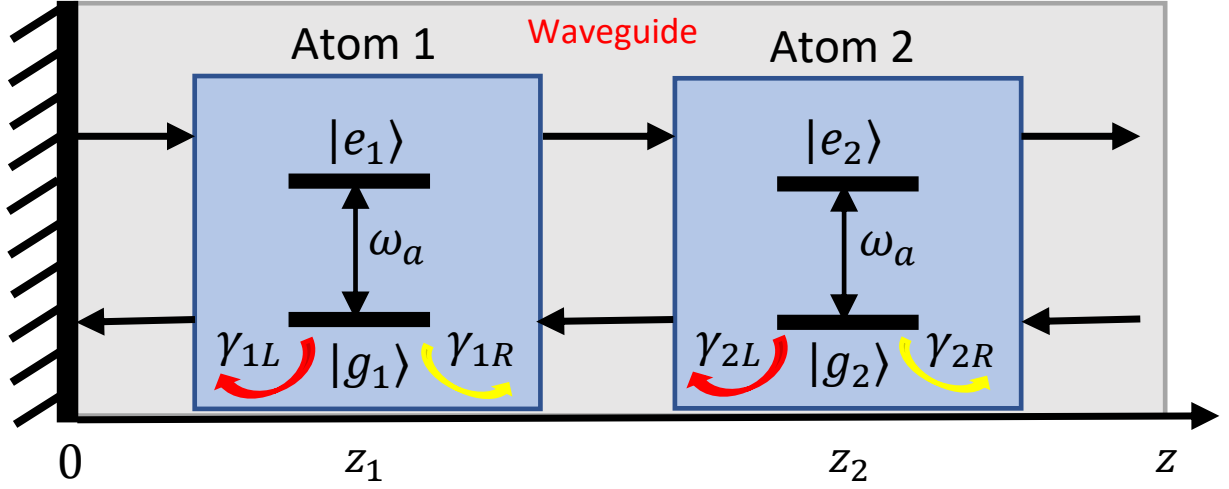


Figure 1: A quantum coherent feedback control scheme where two atoms are coupled with a semi-infinite waveguide.

the right-propagating direction leaves the system.

The following assumption is used in the frequency domain analysis.

Assumption 1 *Initially, both of the two atoms are in their excited states, the waveguide is empty, and there are no external drives. Thus, there are at most two excitations in the whole system.*

The free Hamiltonian of the system reads

$$H_0 = \sum_{j=1,2} \omega_a \sigma_j^+ \sigma_j^- + \int \omega d_k^\dagger d_k dk, \quad (1)$$

where the first component represents the atomic Hamiltonian, and the second component represents the fields in the waveguide, respectively. Here, $\sigma_j^- = |g_j\rangle\langle e_j|$ and $\sigma_j^+ = |e_j\rangle\langle g_j|$ are the lowering and raising operators of the j th atom respectively, $d_k(d_k^\dagger)$ are the annihilation(creation) operators of the propagating waveguide modes, $\omega = ck$ and c is the velocity of the field in the waveguide.

The interaction Hamiltonian between the atoms and the waveguide in the interaction picture is (Regidor et al., 2021; Domokos et al., 2002; Dorner and Zoller, 2002; Pichler and Zoller, 2016; Zhang et al., 2020)

$$H_I = i \sum_{j=1,2} \int \left[\left(d_k^\dagger \sigma_j^- \gamma_{jR} e^{-i\omega z_j/c} e^{-i\Phi/2} e^{i(\omega-\omega_a)t} - d_k^\dagger \sigma_j^- \gamma_{jL} e^{i\omega z_j/c} e^{i\Phi/2} e^{i(\omega-\omega_a)t} \right) - \text{H.c.} \right] dk, \quad (2)$$

where Φ is the phase induced by the mirror reflection which is experimentally small (Bradford and Shen, 2013), $d_k^\dagger \sigma_j^-$ represents that an excited atom at z_j can emit photon with the mode k via decaying to its ground state, and H.c. denotes Hermitian conjugate representing the reverse process. The continuous coupling modes between the atoms

and the waveguide are integrated within $[0, +\infty)$ in this paper. Denoting $\tilde{z}_j = z_j + \Phi/2k$, then the above interaction Hamiltonian H_I can be re-written as

$$H_I = i \sum_{j=1,2} \int \left[(d_k^\dagger \sigma_j^- \gamma_{jR} e^{-i\omega \tilde{z}_j/c} e^{i(\omega-\omega_a)t} - d_k^\dagger \sigma_j^- \gamma_{jL} e^{i\omega \tilde{z}_j/c} e^{i(\omega-\omega_a)t}) - \text{H.c.} \right] dk. \quad (3)$$

That is, the phase shift Φ vanishes under the global translation of the atoms' positions. With slight abuse of notation or take Φ as zero, we still use z_j instead of \tilde{z}_j for simplicity, the interaction Hamiltonian in the interaction picture can be further re-written as

$$H_I = \sum_{j=1,2} \int \left[g_{kj} d_k^\dagger \sigma_j^- + g_{kj}^* d_k \sigma_j^+ \right] dk, \quad (4)$$

where

$$g_{kj}(k, t, z) \triangleq i (\gamma_{jR} e^{-i\omega z_j/c} - \gamma_{jL} e^{i\omega z_j/c}) e^{i(\omega-\omega_a)t}. \quad (5)$$

When the couplings between the atoms and the waveguide are *nonchiral*, namely $\gamma_{jR} = \gamma_{jL} \equiv \gamma_j$ with $j = 1, 2$, the coupling strength in Eq. (5) reduces to $g_{kj} = 2\gamma_j \sin(kz_j) e^{i(\omega-\omega_a)t}$.

According to **Assumption 1**, the whole system has two excitations, hence the state of coherent feedback network is

$$|\Psi(t)\rangle = c_{ee}(t) |e_1, e_2, \{0\}\rangle + \int c_{egk}(t, k) |e_1, g_2, \{k\}\rangle dk + \int c_{gek}(t, k) |g_1, e_2, \{k\}\rangle dk + \int c_{kk}(k_1, k_2, t) |g_1, g_2, \{k_1\}\{k_2\}\rangle dk_1 dk_2. \quad (6)$$

Here, $|e_1, e_2, \{0\}\rangle$ means that both atoms are in the excited state and there are no photons in the waveguide, $|e_1, g_2, \{k\}\rangle$ indicates that the first atom is in the excited state, the second atom is in the ground state, and there is one photon in the waveguide, $|g_1, e_2, \{k\}\rangle$ means that the first atom is in the ground state, the second atom is in the excited state and there is one photon in the waveguide, and finally, $|g_1, g_2, \{k_1\}\{k_2\}\rangle$ represents that both atoms are in the ground state and there are two photons in the waveguide. $c_{ee}(t)$, $c_{egk}(t, k)$, $c_{gek}(t, k)$, and $c_{kk}(k_1, k_2, t)$ are the quantum state amplitudes, respectively.

Solving the Schrödinger equation in the interaction picture,

$$\frac{d}{dt} |\Psi(t)\rangle = -iH_I |\Psi(t)\rangle, \quad (7)$$

with the interaction Hamiltonian in Eq. (4) and the ansatz in Eq. (6), yields a system of integro-differential equations for the amplitudes

$$\begin{cases} \dot{c}_{ee}(t) = -i \int c_{egk}(t, k) g_{k2t}^*(k, t, z_2) dk - i \int c_{gek}(t, k) g_{k1t}^*(k, t, z_1) dk, & (8a) \\ \dot{c}_{egk}(t, k) = -i c_{ee}(t) g_{k2t}(k, t, z_2) - i \int c_{kk}(k, k_1, t) g_{k1t}^*(k_1, t, z_1) dk_1, & (8b) \\ \dot{c}_{gek}(t, k) = -i c_{ee}(t) g_{k1t}(k, t, z_1) - i \int c_{kk}(k, k_1, t) g_{k2t}^*(k_1, t, z_2) dk_1, & (8c) \\ \dot{c}_{kk}(k_1, k_2, t) = -i c_{egk}(t, k_1) g_{k1t}(k_2, t, z_1) - i c_{gek}(t, k_2) g_{k1t}(k_1, t, z_1) \\ \quad - i c_{gek}(t, k_1) g_{k2t}(k_2, t, z_2) - i c_{gek}(t, k_2) g_{k2t}(k_1, t, z_2). & (8d) \end{cases}$$

The physical interpretation of Eq. (8) is as follows. Eq. (8a) means that if one of the two atoms is in the excited state while the other is in the ground state, then both of two atoms can be in the excited state by absorbing one photon from the waveguide. Conversely, the first item of the right-hand side of Eq. (8b) and Eq. (8c) indicates that when the two atoms are in the excited state, one atom can emit a photon into the waveguide and decay to the ground state; whereas the second item describes that one atom can absorb one photon from the waveguide when both of the two atoms are in the ground state. Eq. (8d) means that when only one of the two atoms is in the excited state, the excited atom can emit a photon into the waveguide, then both atoms are in the ground state and there are two photons in the waveguide.

According to the calculations in **Appendix A**, Eq. (8a) can be rewritten as

$$\begin{aligned} \dot{c}_{ee}(t) = & -\frac{\gamma_{1R}^2 + \gamma_{1L}^2 + \gamma_{2R}^2 + \gamma_{2L}^2}{2} c_{ee}(t) \\ & + \gamma_{1L}\gamma_{1R}c_{ee}\left(t - \frac{2z_1}{c}\right) e^{i\omega_a \frac{2z_1}{c}} + \gamma_{2L}\gamma_{2R}c_{ee}\left(t - \frac{2z_2}{c}\right) e^{i\omega_a \frac{2z_2}{c}}, \end{aligned} \quad (9)$$

which explicitly demonstrates the influence of the round-trip delay between the atoms and the terminal mirror $2z_j/c$ with $j = 1, 2$. Similarly, Eq. (8b) can be rewritten as

$$\begin{aligned} \dot{c}_{egk}(t, k) = & -\frac{\gamma_{1R}^2 + \gamma_{1L}^2}{2} c_{egk}(t, k) - ic_{ee}(t)g_{k2l}(k, t, z_2) + \gamma_{1L}\gamma_{1R}c_{egk}\left(t - \frac{2z_1}{c}, k\right) e^{i\omega_a \frac{2z_1}{c}} \\ & + \gamma_{1R}\gamma_{2L}c_{gek}\left(t - \frac{z_1 + z_2}{c}, k\right) e^{i\omega_a \frac{z_1 + z_2}{c}} - \gamma_{1L}\gamma_{2L}c_{gek}\left(t - \frac{z_2 - z_1}{c}, k\right) e^{i\omega_a \frac{z_2 - z_1}{c}}, \end{aligned} \quad (10)$$

where $(z_1 + z_2)/c$ represents the delay from the second atom at z_2 to the first atom at z_1 after the field is reflected by the mirror, and $(z_2 - z_1)/c$ represents the delay directly from the second atom at z_2 to the first atom at z_1 . Finally, Eq. (8c) can be rewritten as

$$\begin{aligned} \dot{c}_{gek}(t, k) = & -\frac{\gamma_{2R}^2 + \gamma_{2L}^2}{2} c_{gek}(t, k) - ic_{ee}(t)g_{k1l}(k, t, z_1) + \gamma_{2L}\gamma_{2R}c_{gek}\left(t - \frac{2z_2}{c}, k\right) e^{i\omega_a \frac{2z_2}{c}} \\ & + \gamma_{1L}\gamma_{2R}c_{gek}\left(t - \frac{z_1 + z_2}{c}, k\right) e^{i\omega_a \frac{z_1 + z_2}{c}} - \gamma_{1R}\gamma_{2R}c_{gek}\left(t - \frac{z_2 - z_1}{c}, k\right) e^{i\omega_a \frac{z_2 - z_1}{c}}, \end{aligned} \quad (11)$$

where $(z_1 + z_2)/c$ and $(z_2 - z_1)/c$ represent the delay from the first atom at z_1 to the second atom at z_2 via the path reflected by the mirror or direct transmission, respectively.

In particular, if we take $\gamma_{jL} = \gamma_{jR}$ for $j = 1, 2$, the above equations reduce to the nonchiral coupling circumstance between the atoms and the waveguide.

For simplicity, denote

$$\gamma_{RL} = \frac{\gamma_{1R}^2 + \gamma_{1L}^2 + \gamma_{2R}^2 + \gamma_{2L}^2}{2}, \quad \mathbf{g}_j = \gamma_{jL}\gamma_{jR}, \quad \tau_j = \frac{2z_j}{c}, \quad (12)$$

where $j = 1, 2$. Clearly, $\gamma_{RL} \geq \mathbf{g}_1 + \mathbf{g}_2$, and the equality holds only when $\gamma_{1L} = \gamma_{1R}$ and $\gamma_{2L} = \gamma_{2R}$.

Applying the Laplace transformation to both sides of Eq. (9), we get

$$C_{ee}(s) = \frac{c_{ee}(0)}{s + \gamma_{RL} - \mathbf{g}_1 e^{i\omega_a \tau_1} e^{-\tau_1 s} - \mathbf{g}_2 e^{i\omega_a \tau_2} e^{-\tau_2 s}}. \quad (13)$$

Next, we investigate the dynamics of the coherent feedback network based on the following assumption.

Assumption 2 The resonant frequency of the atoms satisfies $\omega_a \gg 1$, and the locations of atoms satisfy $z_j \ll c$, $j = 1, 2$.

The inverse Laplace transformation of Eq. (13) is taken by integrating on the positive half of the complex plane close to the imaginary axis. By **Assumption 2**, $e^{-2z_1 s/c} \approx 1$ and $e^{-2z_2 s/c} \approx 1$. Consequently, the amplitude $c_{ee}(t)$ can be approximated as

$$\begin{aligned} c_{ee}(t) &\approx e^{-\left[\gamma_{RL} - \gamma_{1L}\gamma_{1R}e^{i\omega_a \frac{2z_1}{c}} - \gamma_{2L}\gamma_{2R}e^{i\omega_a \frac{2z_2}{c}}\right]t} \\ &= e^{-\left[\gamma_{RL} + \gamma_{1L}\gamma_{1R} \cos\left(\omega_a \frac{2z_1}{c}\right) + \gamma_{2L}\gamma_{2R} \cos\left(\omega_a \frac{2z_2}{c}\right)\right]t} \\ &\quad e^{i\gamma_{1L}\gamma_{1R} \sin\left(\omega_a \frac{2z_1}{c}\right)t} e^{i\gamma_{2L}\gamma_{2R} \sin\left(\omega_a \frac{2z_2}{c}\right)t}. \end{aligned} \quad (14)$$

Because $\omega_a \gg 1$, even when $z_j \ll c$, the value $\omega_a z_j/c$ with $j = 1, 2$ varies in the interval $[0, n\pi]$ for some positive integer n . Consequently, the quantum coherent feedback network dynamics can be distinctly influenced by z_j , which is studied in detail in the following subsections.

2.1. Control the photon number in the waveguide by means of delay and chiral couplings

Based on the delay-dependent control equations (9,10,11), the number of photons in the waveguide can be two, one or zero according to the parameter settings, as given in **Theorems 1-3**.

Theorem 1 Under **Assumption 2**, $\lim_{t \rightarrow \infty} c_{ee}(t) = 0$ when the coupling between the waveguide and at least one of the two atoms is chiral.

Proof When $\gamma_{jL} \neq \gamma_{jR}$ for $j = 1$ or 2 ,

$$\begin{aligned} \gamma_{RL} > \gamma_{1L}\gamma_{1R} + \gamma_{2L}\gamma_{2R} &\geq \gamma_{1L}\gamma_{1R} \cos\left(\omega_a \frac{2z_1}{c}\right) \\ &\quad + \gamma_{2L}\gamma_{2R} \cos\left(\omega_a \frac{2z_2}{c}\right). \end{aligned} \quad (15)$$

Thus for arbitrary γ_{jL} , γ_{jR} and z_j ,

$$-\gamma_{RL} + \gamma_{1L}\gamma_{1R} \cos\left(\omega_a \frac{2z_1}{c}\right) + \gamma_{2L}\gamma_{2R} \cos\left(\omega_a \frac{2z_2}{c}\right) < 0. \quad (16)$$

Then by Eq. (14), $\lim_{t \rightarrow \infty} c_{ee}(t) = 0$. □

Let $|c_{e1}(t)|^2$ (resp. $|c_{e2}(t)|^2$) denote the population that the first (resp. second) atom is in the excited state. Then

$$\begin{cases} |c_{e1}(t)|^2 = |c_{ee}(t)|^2 + \int |c_{egk}(t, k)|^2 dk, \\ |c_{e2}(t)|^2 = |c_{ee}(t)|^2 + \int |c_{gek}(t, k)|^2 dk. \end{cases} \quad (17)$$

In the numerical simulations given in Fig. 2 below, $\gamma_{jR} = 2\gamma_{jL} = 0.5$, $\omega_a = 50$, $z_1 = 0.1$, $z_2 = 0.2$, and $\tau = z_1/c$. Fig. 2(a) clearly shows that the populations of the excited states decay to zero. Moreover, the populations of the

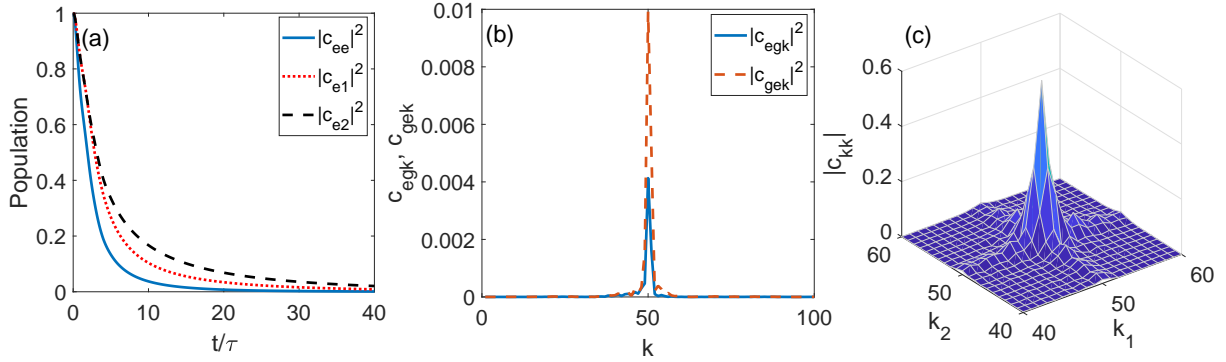


Figure 2: The evolution of two atoms coupled with a waveguide.

single-photon states also decay to zero, as shown in Fig. 2(b) for $t = 40\tau$. As a result, there are two photons in the waveguide and the population of the two-photon state with the modes k_1 and k_2 is shown in Fig. 2(c) for $t = 40\tau$.

For typical chiral interactions between the atoms and the waveguide, by **Theorem 1** asymptotically there are two photons in the waveguide and the atoms are in their ground states. However, under certain extreme conditions, it may happen that there is only one photon in the waveguide and one atom is in the excited state persistently, as given in the following theorem.

Theorem 2 When $\gamma_{1R} = \gamma_{1L}$, $z_1 = n\pi/\omega_a \ll c$ for some positive integer n , $z_2 \ll c$, $\gamma_{2R} > \gamma_{2L} = 0$ or $\gamma_{2L} > \gamma_{2R} = 0$, the first atom holds a significant amount of excitation and the second atom decays to the ground state.

Proof We look at the case $\gamma_{2L} > \gamma_{2R} = 0$. The other case $\gamma_{2L} > \gamma_{2R} = 0$ can be proved similarly. Under the assumptions in **Theorem 2**, Eqs. (9,10,11) become

$$\begin{cases} \dot{c}_{ee}(t) = -\frac{\gamma_{2L}^2 + \gamma_{1R}^2 + \gamma_{1L}^2}{2}c_{ee}(t) + \gamma_{1L}\gamma_{1R}c_{ee}\left(t - \frac{2z_1}{c}\right)e^{i\omega_a\frac{2z_1}{c}}, \\ \dot{c}_{gek}(t, k) = -ic_{ee}(t)g_{k1t}(k, t, z_1) - \frac{\gamma_{2L}^2}{2}c_{gek}(t, k), \\ \dot{c}_{egk}(t, k) = -ic_{ee}(t)g_{k2t}(k, t, z_2) - \frac{\gamma_{1R}^2 + \gamma_{1L}^2}{2}c_{egk}(t, k) + \gamma_{1L}\gamma_{1R}c_{egk}\left(t - \frac{2z_1}{c}, k\right)e^{i\omega_a\frac{2z_1}{c}} \\ + \gamma_{1R}\gamma_{2L}c_{gek}\left(t - \frac{z_1 + z_2}{c}, k\right)e^{i\omega_a\frac{z_1 + z_2}{c}} - \gamma_{1L}\gamma_{2L}c_{gek}\left(t - \frac{z_2 - z_1}{c}, k\right)e^{i\omega_a\frac{z_2 - z_1}{c}}. \end{cases} \quad (18)$$

Applying the Laplace transformation to the first two equations of (18) yields

$$C_{ee}(s) = \frac{1}{s + \frac{\gamma_{2L}^2 + \gamma_{1R}^2 + \gamma_{1L}^2}{2} - \gamma_{1L}\gamma_{1R}e^{i\omega_a\frac{2z_1}{c}}e^{-\frac{2z_1}{c}s}}. \quad (19)$$

By the final-value theorem,

$$\begin{aligned} \lim_{t \rightarrow \infty} c_{ee}(t) &= \lim_{s \rightarrow 0} sC_{ee}(s) \\ &= \lim_{s \rightarrow 0} \frac{s}{s + \frac{\gamma_{2L}^2 + \gamma_{1R}^2 + \gamma_{1L}^2}{2} - \gamma_{1L}\gamma_{1R}e^{i\omega_a\frac{2z_1}{c}}e^{-\frac{2z_1}{c}s}} = 0. \end{aligned} \quad (20)$$

As a result, in the long-time limit, $\dot{c}_{gek}(t, k) \approx -(\gamma_{2L}^2/2)c_{gek}(t, k)$, and hence $\lim_{t \rightarrow \infty} c_{gek}(t, k) = 0$. Thus, if $t > t_1$ for some t_1 large enough, $c_{ee}(t) \approx 0$ and $c_{gek}(t, k) \approx 0$. In this case, when $z_1 = n\pi/\omega_a$, the third equation of Eq. (18) can be simplified when $t > t_1$ as

$$\dot{c}_{gek}(t, k) \approx -\frac{\gamma_{1R}^2 + \gamma_{1L}^2}{2}c_{gek}(t, k) + \gamma_{1L}\gamma_{1R}c_{gek}\left(t - \frac{2z_1}{c}, k\right)e^{i\omega_a \frac{2z_1}{c}}. \quad (21)$$

The Laplace transformation of Eq. (21) reads

$$\begin{aligned} & sC_{egk}(s, k) - c_{egk}(t_1, k) \\ &= -\frac{\gamma_{1R}^2 + \gamma_{1L}^2}{2}C_{egk}(s, k) + \gamma_{1L}\gamma_{1R}C_{egk}(s, k)e^{-\frac{2z_1 s}{c}}e^{i\omega_a \frac{2z_1}{c}} \\ &\approx -\frac{\gamma_{1R}^2 + \gamma_{1L}^2}{2}C_{egk}(s, k) + \gamma_{1L}\gamma_{1R}C_{egk}(s, k)e^{i\omega_a \frac{2z_1}{c}}, \end{aligned} \quad (22)$$

which yields

$$C_{egk}(s, k) \approx \frac{c_{egk}(t_1, k)}{s + \frac{\gamma_{1R}^2 + \gamma_{1L}^2}{2} - \gamma_{1L}\gamma_{1R}e^{i\omega_a \frac{2z_1}{c}}}. \quad (23)$$

Consequently, when $\gamma_{1L} = \gamma_{1R}$ and $\omega_a z_1/c = n\pi$, we have $c_{gek}(t, k) \approx c_{gek}(t_1, k)$. \square

The numerical simulations in Fig. 3 is used to demonstrate **Theorem 2**, where $z_1 = \pi/\omega_a$, $z_2 = 2\pi/\omega_a$, $\gamma_{1L} = \gamma_{1R} = 0.25$, $\gamma_{2L} = 0.5$, $\gamma_{2R} = 0$, and $\omega_a = 50$. As shown in Fig. 3(a), the population $|c_{ee}(t)|^2$ converges to zero, while the population $|c_{e1}(t)|^2$ that the first atom is excited remains around 0.86. As can be seen in Fig. 3(b), the amplitude of the single-photon state c_{egk} approximates a bump function at $\omega = \omega_a$ and $t = 40\tau$. Finally, as shown in Fig. 3(c), there are no observable two-photon state in the waveguide for $t = 40\tau$.

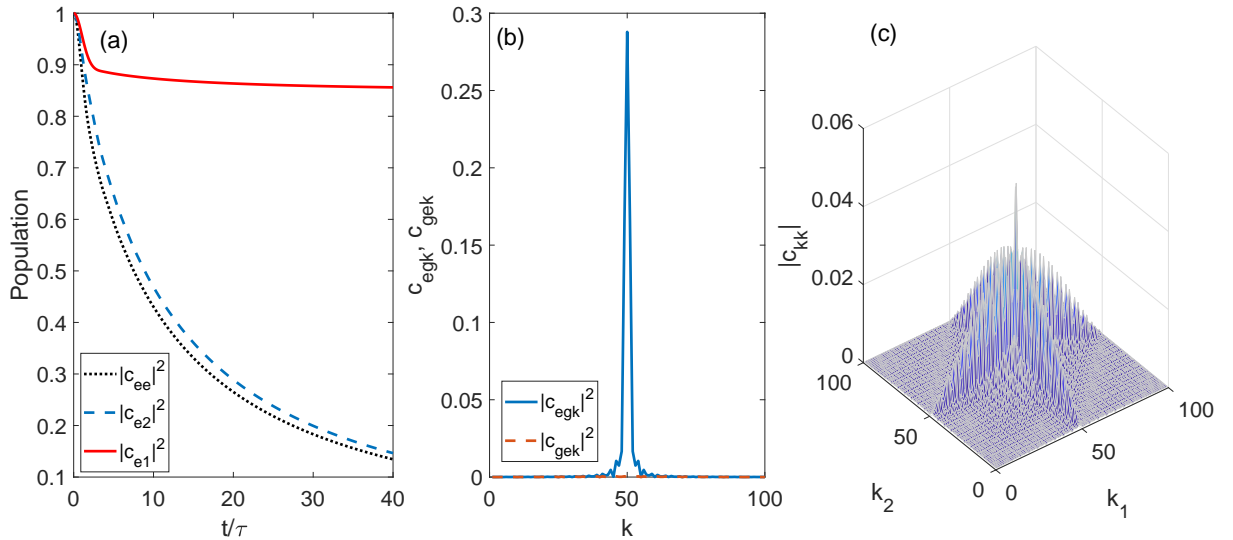


Figure 3: Control performance of the generation of the single photon state.

For the nonchiral case, we have the following result.

Theorem 3 For the nonchiral waveguide, when $z_j = n\pi/\omega_a \ll c$, where $n = 0, 1, 2, \dots$, $j = 1, 2$, $c_{ee}(t) \approx 1$.

Proof For the nonchiral waveguide, $\gamma_{jR} = \gamma_{jL}$. When $z_j = n\pi/\omega_a \ll c$ with $n = 0, 1, 2, \dots$ and $j = 1, 2$, it is easy to show that $-\gamma_{RL} + \gamma_{1L}\gamma_{1R} \cos(2\omega_a z_1/c) + \gamma_{2L}\gamma_{2R} \cos(2\omega_a z_2/c) \approx 0$ due to $\sin(2\omega_a z_j/c) = 0$ and $\cos(2\omega_a z_j/c) = 1$ in Eq. (14). As a result, $c_{ee}(t) \approx 1$. \square

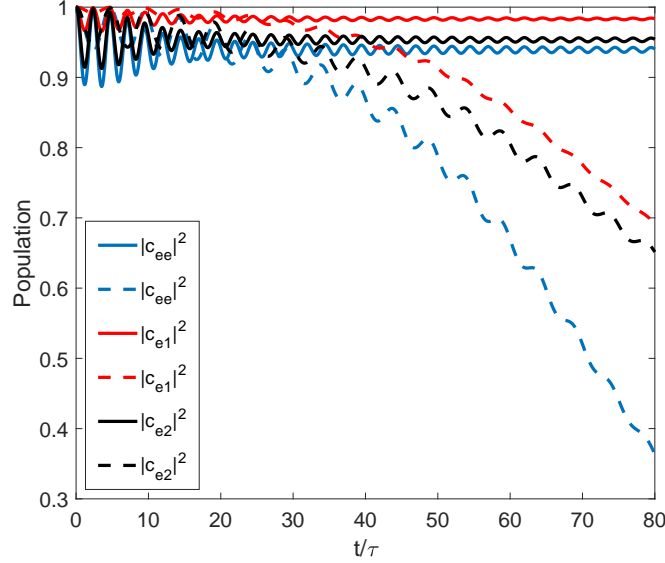


Figure 4: Comparison of the influence of atoms' locations on the excited states.

As compared in Fig.4, the solid lines represent the simulations when $z_1 = \pi/\omega_a$ and $z_2 = 2\pi/\omega_a$, and the dashed lines represent that $z_1 = \pi/2\omega_a$ and $z_2 = 3\pi/2\omega_a$. In both cases, $\omega_a = 50$, $\gamma_{jR} = \gamma_{jL} = 0.5$. The comparisons agree with the conclusions in **Theorem 1** and **Theorem 3**. That is, when the locations of the two charily coupled atoms are $z_j = n\pi/\omega_a$, $n = 1, 2, \dots$, $j = 1, 2$, which is the case for the solid lines in Fig.4, the two atoms maintain their excited states due to the coherent feedback interactions.

Remark 1 The conclusion of **Theorem 2** and **Theorem 3** reveals that the coherent feedback network can maintain either one excited atom or both excited atoms by properly tuning the location of atoms and the chiral coupling strengths between the atoms and waveguide. In **Theorem 2**, there is one excited atom and a photon packet is in the waveguide, this is often called the atom-photon bound state, which has been introduced based on the coherent feedback network that one two-level atom is nonchirally coupled with a semi-infinite waveguide in (Tufarelli et al., 2013). In **Theorem 3**, both atoms are excited while there are no photons in the waveguide, which constructs a dark state of the system and can be regarded as a generalization of the one-atom circumstance in (Qiao and Sun, 2019). The formation of dark states is physically important because it can enhance the lifetime of the qubits by elongating the duration of the excited states. This also provides a new method to generate trapped excited quantum states through coherent feedback designs.

In summary, for the coherent feedback network where two atoms are coupled with a semi-infinite waveguide, the number of photons in the waveguide can be controlled by tuning the chirally coupling strengths between the atoms and waveguide as well as the locations of the atoms, which makes it possible to generate zero-photon, one-photon and two-photon states in the waveguide.

2.2. The relationship between delay and the coherent feedback network model

In this subsection, we study the relationship between delay and atomic dynamics from two perspectives; one is based on a quasi-polynomial model by applying the Laplace transformation to the linear control equation with delays, and the other is based on the master equation under the Markovian approximation, where the delays play the role of phase modulations.

2.2.1. Quasi-polynomial model

Consider the delay dependent Eq. (9), which can be complex-valued for most parameter settings of z_1, z_2 and γ_{jL} , γ_{jR} with $j = 1, 2$. We rewrite this equation by denoting the real and imaginary parts of $c_{ee}(t)$ as real-valued functions $c_{ee}^R(t)$ and $c_{ee}^I(t)$, respectively. Namely, $c_{ee}(t) = c_{ee}^R(t) + ic_{ee}^I(t)$. According to Eq. (12), we have

$$\begin{cases} \dot{c}_{ee}^R(t) = -\gamma_{RL}c_{ee}^R(t) + \mathbf{g}_1c_{ee}^R(t - \tau_1) \cos(\omega_a\tau_1) \\ \quad - \mathbf{g}_1c_{ee}^I(t - \tau_1) \sin(\omega_a\tau_1) + \mathbf{g}_2c_{ee}^R(t - \tau_2) \cos(\omega_a\tau_2) \\ \quad - \mathbf{g}_2c_{ee}^I(t - \tau_2) \sin(\omega_a\tau_2), \\ \dot{c}_{ee}^I(t) = -\gamma_{RL}c_{ee}^I(t) + \mathbf{g}_1c_{ee}^R(t - \tau_1) \sin(\omega_a\tau_1) \\ \quad + \mathbf{g}_1c_{ee}^I(t - \tau_1) \cos(\omega_a\tau_1) + \mathbf{g}_2c_{ee}^R(t - \tau_2) \sin(\omega_a\tau_2) \\ \quad + \mathbf{g}_2c_{ee}^I(t - \tau_2) \cos(\omega_a\tau_2), \end{cases} \quad (24a)$$

$$\begin{cases} \dot{c}_{ee}^R(t) = -\gamma_{RL}c_{ee}^R(t) + \mathbf{g}_1c_{ee}^R(t - \tau_1) \cos(\omega_a\tau_1) \\ \quad - \mathbf{g}_1c_{ee}^I(t - \tau_1) \sin(\omega_a\tau_1) + \mathbf{g}_2c_{ee}^R(t - \tau_2) \cos(\omega_a\tau_2) \\ \quad - \mathbf{g}_2c_{ee}^I(t - \tau_2) \sin(\omega_a\tau_2), \\ \dot{c}_{ee}^I(t) = -\gamma_{RL}c_{ee}^I(t) + \mathbf{g}_1c_{ee}^R(t - \tau_1) \sin(\omega_a\tau_1) \\ \quad + \mathbf{g}_1c_{ee}^I(t - \tau_1) \cos(\omega_a\tau_1) + \mathbf{g}_2c_{ee}^R(t - \tau_2) \sin(\omega_a\tau_2) \\ \quad + \mathbf{g}_2c_{ee}^I(t - \tau_2) \cos(\omega_a\tau_2), \end{cases} \quad (24b)$$

according to the definition of variables in Eq. (12). We treat the delay-dependent components

$$\begin{cases} u_1(t) = c_{ee}^R(t - \tau_1), \\ v_1(t) = c_{ee}^I(t - \tau_1), \\ u_2(t) = c_{ee}^R(t - \tau_2), \\ v_2(t) = c_{ee}^I(t - \tau_2), \end{cases} \quad (25)$$

as the controls with delays. Denote $\mathbf{x}(t) = [c_{ee}^R(t), c_{ee}^I(t)]^T$ with T representing the transpose of a vector or matrix, $\mathbf{u}_1(t) = [u_1(t), v_1(t)]^T$ and $\mathbf{u}_2(t) = [u_2(t), v_2(t)]^T$. Then Eq. (24) can be rewritten with a format a linear control system as

$$\dot{\mathbf{x}}(t) = A\mathbf{x}(t) + B_1\mathbf{u}_1(t) + B_2\mathbf{u}_2(t), \quad (26)$$

where

$$A = \begin{bmatrix} -\gamma_{RL} & 0 \\ 0 & -\gamma_{RL} \end{bmatrix}, \quad (27)$$

$$B_j = \begin{bmatrix} \mathbf{g}_j \cos(\omega_a \tau_j) & -\mathbf{g}_j \sin(\omega_a \tau_j) \\ \mathbf{g}_j \sin(\omega_a \tau_j) & \mathbf{g}_j \cos(\omega_a \tau_j) \end{bmatrix}, \quad j = 1, 2. \quad (28)$$

It can be readily shown that the characteristic equation of the system (26) reads (Angulo et al., 2019)

$$\begin{aligned} \Delta_c(s) &= |sI - A - B_1 e^{-\tau_1 s} - B_2 e^{-\tau_2 s}| \\ &= \begin{vmatrix} s + \gamma_{RL} - \sum_j \mathbf{b}_j e^{-\tau_j s} & \sum_j \tilde{\mathbf{b}}_j e^{-\tau_j s} \\ -\sum_j \tilde{\mathbf{b}}_j e^{-\tau_j s} & s + \gamma_{RL} - \sum_j \mathbf{b}_j e^{-\tau_j s} \end{vmatrix} \\ &= \left(s + \gamma_{RL} - \sum_j \mathbf{b}_j e^{-\tau_j s} \right)^2 + \left(\sum_j \tilde{\mathbf{b}}_j e^{-\tau_j s} \right)^2, \end{aligned} \quad (29)$$

where $\mathbf{b}_j = \mathbf{g}_j \cos(\omega_a \tau_j) = \gamma_{jL} \gamma_{jR} \cos(\omega_a \tau_j)$ and $\tilde{\mathbf{b}}_j = \mathbf{g}_j \sin(\omega_a \tau_j)$.

Clearly, when $\tau_j \approx 0$ for $j = 1, 2$, Eq. (29) can be approximated as

$$\begin{aligned} \Delta_c(s) &\approx \left(s + \gamma_{RL} - \sum_j \mathbf{b}_j \right)^2 + \left(\sum_j \tilde{\mathbf{b}}_j \right)^2 \\ &= \left[s + \gamma_{RL} - \sum_j (\mathbf{b}_j - i\tilde{\mathbf{b}}_j) \right] \left[s + \gamma_{RL} - \sum_j (\mathbf{b}_j + i\tilde{\mathbf{b}}_j) \right]. \end{aligned} \quad (30)$$

In particular, for the special case that $\sin(\omega_a \tau_j) = 0$, we get $\tilde{\mathbf{b}}_j = 0$, and consequently $\mathbf{x}(t)$ is exponentially stable when the delays are small, which agrees with the conclusion in **Theorems 1-3**. On the other hand, when $\sin(\omega_a \tau_j) \neq 0$, the real parts of the roots of Eq. (30) are both negative, and thus $\mathbf{x}(t)$ converges to zero too.

For the general case of τ_j , Eq. (29) can be rewritten as the following quasi-polynomial (Angulo et al., 2019)

$$\begin{aligned} \Delta_c(s) &= \left(s + \gamma_{RL} - \sum_j \mathbf{b}_j e^{-\tau_j s} \right)^2 + \left(\sum_j \tilde{\mathbf{b}}_j e^{-\tau_j s} \right)^2 \\ &= (s + \gamma_{RL})^2 - 2 \sum_j \mathbf{b}_j (s + \gamma_{RL}) e^{-\tau_j s} + \left(\sum_j \mathbf{b}_j e^{-\tau_j s} \right)^2 + \left(\sum_j \tilde{\mathbf{b}}_j e^{-\tau_j s} \right)^2 \\ &= \sum_{q=0}^2 \sum_{p=0}^5 a_{qp} s^q e^{-\Gamma_p s}, \end{aligned} \quad (31)$$

where $\Gamma_0 = 0$, $\Gamma_1 = \tau_1$, $\Gamma_2 = \tau_2$, $\Gamma_3 = 2\tau_1$, $\Gamma_4 = \tau_1 + \tau_2$, $\Gamma_5 = 2\tau_2$. The parameters a_{qp} in Eq. (31) are $a_{20} = 1$, $a_{10} = 2\gamma_{RL}$, $a_{00} = \gamma_{RL}^2$, and we can similarly derive the values of a_{qp} for $p > 0$. For simplicity, we denote

$$\Delta_c(s) = \sum_{p=0}^5 L_p(s) e^{-\Gamma_p s}, \quad (32)$$

with $L_p(s) = \sum_{q=0}^2 a_{qp} s^q$. Because $\tau_2 \geq \tau_1$, $0 \leq \Gamma_p / \Gamma_5 \leq (\tau_1 + \tau_2) / 2\tau_2 \leq 1$ for $p = 0, 1, 2, 3, 4$. The quasi-polynomials in Eqs. (31,32) will be used to analyze the quantum coherent feedback control dynamics, in combination with the master equation given below.

2.2.2. Master equation representation

Under the Markovian approximation, the transmission delay in the waveguide is interpreted as a phase, and the quantum state dynamics is given by the master equation (Kockum et al., 2018; Soro and Kockum, 2022)

$$\dot{\rho}(t) = -i \left[\sum_{j=1,2} H_{\text{eff}}^{(j)} + H_{\text{eff}}^I, \rho(t) \right] + \sum_{j=1,2} \tilde{\Gamma}_j \mathcal{L}_j[\rho(t)] + \mathcal{D}_{12}[\rho(t)]. \quad (33)$$

Here, the Hamiltonian terms are

$$H_{\text{eff}}^{(j)} = -\gamma_{jL}\gamma_{jR} \sin\left(\omega_a \frac{2z_j}{c}\right) \sigma_j^+ \sigma_j^-, \quad (34)$$

$$\begin{aligned} H_{\text{eff}}^I = & \left(\frac{\gamma_{1L}\gamma_{2L}}{4} + \frac{\gamma_{1R}\gamma_{2R}}{4} \right) \sin\left(\omega_a \frac{z_2 - z_1}{c}\right) \sigma_1^+ \sigma_2^- \\ & - \left(\frac{\gamma_{1L}\gamma_{2R}}{4} + \frac{\gamma_{1R}\gamma_{2L}}{4} \right) \sin\left(\omega_a \frac{z_1 + z_2}{c}\right) \sigma_1^+ \sigma_2^- + \text{H.c.}, \end{aligned} \quad (35)$$

the Lindblad components are

$$\mathcal{L}_j[\rho(t)] = \sigma_j^- \rho(t) \sigma_j^+ - \frac{1}{2} \rho(t) \sigma_j^+ \sigma_j^- - \frac{1}{2} \sigma_j^+ \sigma_j^- \rho(t) \quad (36)$$

with coefficient (Kockum et al., 2018)

$$\tilde{\Gamma}_j = \frac{\gamma_{jR}^2 + \gamma_{jL}^2}{2} - \gamma_{jL}\gamma_{jR} \cos\left(\omega_a \frac{2z_j}{c}\right), \quad (37)$$

and

$$\begin{aligned} & \mathcal{D}_{12}[\rho(t)] \\ = & \Gamma_{\text{coll}} \left[\sigma_1^- \rho(t) \sigma_2^+ - \frac{1}{2} \rho(t) \sigma_1^+ \sigma_2^- - \frac{1}{2} \sigma_1^+ \sigma_2^- \rho(t) + \text{H.c.} \right], \end{aligned} \quad (38)$$

which represents the collective relaxation process of the two atoms (Kockum et al., 2018), where

$$\begin{aligned} \Gamma_{\text{coll}} = & (\gamma_{1R}\gamma_{2R} + \gamma_{1L}\gamma_{2L}) \cos\left(\omega_a \frac{z_2 - z_1}{c}\right) \\ & - (\gamma_{1L}\gamma_{2R} + \gamma_{1R}\gamma_{2L}) \cos\left(\omega_a \frac{z_1 + z_2}{c}\right). \end{aligned} \quad (39)$$

In particular, when $\gamma_{jL} = \gamma_{jR}$ for $j = 1, 2$, the master equation (33) reduces to the non-chiral case in (Kockum et al., 2018).

Remark 2 Because initially the two atoms are both excited, in our case it is possible that $\text{Rank}[\rho(t)] = 4$ when $t > 0$, while in (Zhang et al., 2020) for the single-excitation case, $\text{Rank}[\rho(t)] \leq 3$ always holds.

2.3. Atomic dynamics and photon emission analysis

In this subsection, we analyze the atomic dynamics based on the quasi-polynomial model and master equation presented in the preceding subsections.

Theorem 4 The smallest value of the j th atom's independent decay rate $\tilde{\Gamma}_j$ is attained when $z_j = n\pi/\omega_a$, where $n = 1, 2, \dots$.

Proof The j th atom's decay rate $\tilde{\Gamma}_j$ to the waveguide is given in Eq. (37). Clearly, its smallest value for the fixed γ_{jR} and γ_{jL} is reached at $z_j = n\pi/\omega_a$.

According to **Theorem 4**, for fixed coupling strengths between atom and waveguide, the exponential stability for quantum systems with coherent feedback is the worst when $z_j = n\pi/\omega_a$. In other words, if the amplitudes for the atom's excited state exponentially converges to zero when $z_j = n\pi/\omega_a$, then it will certainly exponentially converge to zero for arbitrary delays. Thus, it suffices to study the stability when $z_j = n\pi/\omega_a$. In this parameter setting, the control equation of $c_{ee}(t)$ reduces to a real-value equation as $c_{ee}^I(t) \equiv 0$ in Eq. (24).

When $z_j = n\pi/\omega_a$ and $z_2/z_1 = m$, where m is an integer, Eq. (24a) is simplified as

$$\begin{aligned} \dot{c}_{ee}^R(t) = & -\gamma_{RL}c_{ee}^R(t) + \mathbf{g}_1c_{ee}^R(t - \tau_1)\cos(\omega_a\tau_1) \\ & + \mathbf{g}_2c_{ee}^R(t - \tau_2)\cos(\omega_a\tau_2). \end{aligned} \quad (40)$$

Denote $\tilde{z} = e^{-z_1 s}$, and define the quasi-polynomial function $F(\tilde{z}) = \sum_{p=0}^2 F_p \tilde{z}^p$, according to the general representation in Eq. (31).

Based on **Theorem 4**, the following **Theorem 5** gives the condition when the systems is delay-independent stable.

Theorem 5 (Kamen, 1980, 1982) When $z_2/z_1 = m$, where m is an integer, Eq. (24a) is delay-independent stable if

1) the quasi-polynomial

$$P(s, e^{i\omega}) \neq 0, \quad \text{Re}(s) \geq 0, \omega \in [0, 2\pi],$$

where $P(s, e^{-\tau_1 s})$ is the quasi-polynomial defined according to Eq. (24a), or

2) the real part of all the eigenvalues of $F(\tilde{z})$ is negative.

Furthermore, the stability of the coherent feedback control network when the atoms are chirally coupled with the waveguide is given by the following theorem.

Theorem 6 When the couplings are chiral, the coherent feedback network is exponentially stable independent of delay.

Proof In the master equation (33), if the atoms are chirally coupled with the waveguide, the amplitudes of the Lindblad components $\tilde{\Gamma}_j > 0$ no matter whether the delays are small or large, which means that the atoms exponentially decay to the ground states, independent of delays.

Based on Eq. (33), we have the following result on the spontaneous emission rate of the two-atom network.

Theorem 7 When $\gamma_{1R} = \gamma_{1L}$, $z_1 = n\pi/\omega_a \ll c$ for some positive integer n , there is no collective relaxation between the two atoms, and instead the two atoms emit the coherent field independently to the waveguide.

Proof The proof is straightforward because $\Gamma_{\text{coll}} = 0$ in Eq. (39) when the condition is satisfied.

Remark 3 A special case of **Theorem 7** is **Theorem 2** for the generation of single-photon state in the waveguide. As there is no collective relaxation between the two atoms, the second atom at z_2 emits one photon into the waveguide and decays to its ground state due to its chiral coupling with the waveguide, while the first atom at z_1 remains excited.

To conclude, because there are no external drives applied upon the quantum coherent network, the stability evaluated by the convergence rate of the quantum state amplitudes is related to the spontaneous emission rate of the atoms. This can be equivalently analyzed based on Eq. (14) and Eq. (33), respectively, as detailed below.

On one hand, the two-photon emission rate is determined by the localization of the poles in Eq. (13), or the time-domain representation of the amplitudes that two atoms are excited in Eq. (14). When the delay is small, the spontaneous emission rate can be approximated as $\gamma_{RL} - \gamma_{1L}\gamma_{1R} \cos(2\omega_a z_1/c) - \gamma_{2L}\gamma_{2R} \cos(2\omega_a z_2/c) \geq 0$, as given in Eq. (14). When the delay is large, i.e., $2z_1/c \gg 0$, the spontaneous emission rate is γ_{RL} when $t < 2z_1/c$, and can be re-excited by absorbing the photon in the waveguide when $t > 2z_1/c$.

On the other hand, when the evolution of quantum states is modeled with the master equation (33), and the waveguide is regarded as the environment, the spontaneous emission rate of atoms can be evaluated by the amplitudes of the Lindblad component, namely $\tilde{\Gamma}_j$ in Eq. (37), as analyzed in **Theorems 4** and **6**.

3. Feedback control in the spatial domain

The number of photons in the waveguide can be studied by means of the delay-dependent feedback equations (9-11). However, the spatial distribution of photons in the waveguide can only be studied by modeling in the spatial domain. The Hamiltonian of the waveguide in the frequency domain is given by the second term on the right-hand side of Eq. (1), whose spatial domain counterpart is (Shen and Fan, 2009; Bradford and Shen, 2013)

$$H_w = iv_g \int_0^\infty c_L^\dagger(z) \frac{\partial}{\partial z} c_L(z) dz - iv_g \int_0^\infty c_R^\dagger(z) \frac{\partial}{\partial z} c_R(z) dz, \quad (41)$$

where v_g is the group velocity of the photonic wavepacket in the waveguide, $c_L^\dagger(z)$ and $c_L(z)$ are the creation and annihilation operators for the left-propagating field at the position z , and $c_R^\dagger(z)$ and $c_R(z)$ are those for the right-propagating field. The derivation of Eq. (41) is given in **Appendix B**.

In subsection 3.1, we study the chiral feedback dynamics when there is a single atom coupled with a semi-infinite waveguide. Then we generalize to the two-atom case in subsection 3.2.

3.1. One atom coupled with the waveguide

When there is only the first atom at $z = z_1$ in Fig. 1 coupled with the waveguide, namely $\gamma_{2L} = \gamma_{2R} = 0$, the quantum state for this one-exciton case is

$$|\Psi(t)\rangle = \int_0^\infty \Phi_R(z, t) e^{-i\tilde{\omega}_1 t} |1_z^r, g\rangle dz + \int_0^\infty \left[\Phi_L(z, t) e^{-i\tilde{\omega}_1 t} |1_z^l, g\rangle + c_e(t) e^{-i\tilde{\omega}_2 t} |0, e\rangle \right] dz, \quad (42)$$

where $|1_z^r, g\rangle$ means that the first atom is at the ground state and the right or left-propagating photon can be detected at the position z , $|0, e\rangle$ means that the first atom is excited and the waveguide is empty, $\Phi_R(z, t)$ denotes the amplitude of the right-propagating photon wavepacket at the position z , $\Phi_L(z, t)$ is the amplitude of a left-propagating photon wavepacket, $c_e(t)$ is the amplitude that the first atom is excited, and $\tilde{\omega}_1$ and $\tilde{\omega}_2$ are the eigenfrequencies of the ground and excited state respectively with $\omega_a = \tilde{\omega}_2 - \tilde{\omega}_1$.

The Hamiltonian of the whole quantum system reads

$$H = \tilde{\omega}_1|g\rangle\langle g| + \tilde{\omega}_2|e\rangle\langle e| + H_w + H_m + H_I, \quad (43)$$

where the waveguide Hamiltonian H_w is given in Eq. (41), the mirror Hamiltonian H_m is given by Eq. (B.8) within **Lemma 4** in **Appendix B**, and the interaction Hamiltonian H_I can be derived by transforming from the frequency domain (as in Eq. (4)) to the spatial domain, which is as the format of Eq.(B.5) in **Appendix B**.

Solving the Schrödinger equation $\frac{d}{dt}|\Psi(t)\rangle = -iH|\Psi(t)\rangle$ with H in Eq. (43) and the ansatz $|\Psi(t)\rangle$ in Eq. (42), we get a system of partial differential equations (PDEs) of the form

$$\begin{cases} \dot{c}_e(t) = -[\gamma_{1R}\Phi_R(z_1, t) + \gamma_{1L}\Phi_L(z_1, t)] e^{i\omega_a t}, & (44a) \\ \frac{\partial\Phi_R(z, t)}{\partial t} = -v_g \frac{\partial\Phi_R(z, t)}{\partial z} + 2v_g\delta(z)\Phi_L(z, t)e^{i2kz} \\ \quad + \gamma_{1R}\delta(z - z_1)c_e(t)e^{-i\omega_a t}, & (44b) \\ \frac{\partial\Phi_L(z, t)}{\partial t} = v_g \frac{\partial\Phi_L(z, t)}{\partial z} - 2v_g\delta(z)\Phi_R(z, t)e^{-2ikz} \\ \quad + \gamma_{1L}\delta(z - z_1)c_e(t)e^{-i\omega_a t}, & (44c) \end{cases}$$

where Eq. (44a) means that the excited atom can emit a single photon into the waveguide along the right or left direction, and the probability is determined by the chiral coupling strengths between the atom and the waveguide; Eq. (44b) shows that the right-propagating mode is determined by the reflection of the mirror from the left-propagating mode at $z = 0$, the position of the atom, and the coupling strength between the atom and the waveguide along the right direction; Eq. (44c) further shows that the left-propagating mode can be influenced by the coupling strength between the atom and the waveguide along the left direction.

Remark 4 *One of the advantages of representing the evolution of the quantum system as formula (44) in the spatial domain is that the differential of the excited atomic state is directly represented with the spatial distribution of the photon states rather than their integrations as in Eq. (8).*

The quantum state with one right- or left-propagating photon in the waveguide $\Phi_R(z, t)$ and $\Phi_L(z, t)$ in Eq. (42) can be represented according to the position as

$$\begin{cases} \Phi_R(z, t) = [\Theta(z) - \Theta(z - z_1)]f_r(t - z/c) \\ \quad + \Theta(z - z_1)g_r(t - z/c), & (45a) \\ \Phi_L(z, t) = [\Theta(z) - \Theta(z - z_1)]f_l(t + z/c), & (45b) \end{cases}$$

respectively, where Θ represents the Heaviside step function, $f_r(t - z/c)$ represents the right-propagating photonic mode in the area $0 < z < z_1$, $g_r(t - z/c)$ is that in the area $z > z_1$, and $f_l(t + z/c)$ represents the left-propagating photonic mode in the area $0 < z < z_1$ (Bradford and Shen, 2013).

According to the calculations in **Appendix C**, Eq. (44a) can be written in the delay-dependent form as

$$\dot{c}_e(t) = -\frac{\gamma_{1R}^2 + \gamma_{1L}^2}{2v_g} c_e(t) + \frac{\gamma_{1L}\gamma_{1R}}{v_g} c_e(t - 2z_1/c) e^{i2\omega_a z_1/c}. \quad (46)$$

Let the atom be initialized in the excited state, i.e., $c_e(0) = 1$. Laplace transforming Eq. (46) yields

$$sC_e(s) - 1 = -\frac{\gamma_{1R}^2 + \gamma_{1L}^2}{2} C_e(s) + \gamma_{1L}\gamma_{1R} C_e(s) e^{-2z_1 s/c} e^{i2\omega_a z_1/c}. \quad (47)$$

We have

$$C_e(s) = \frac{1}{s - \gamma_{1L}\gamma_{1R} e^{-2z_1 s/c} e^{i2\omega_a z_1/c} + \frac{\gamma_{1R}^2 + \gamma_{1L}^2}{2}}, \quad (48)$$

which agrees with Eq. (9) with $\gamma_{2R} = \gamma_{2L} = 0$.

Theorem 8 When $\gamma_{1R} = \gamma_{1L}$, and $z_1 = n\pi/\omega_a \ll c$, where n is an integer satisfying that $n\pi/\omega_a \ll c$, the atom at z_1 can be always excited.

Proof When $\gamma_{1R} = \gamma_{1L}$, and $z_1 = n\pi/\omega_a \ll c$, $-\gamma_{1L}\gamma_{1R} e^{-2z_1 s/c} e^{i2\omega_a z_1/c} + (\gamma_{1R}^2 + \gamma_{1L}^2)/2 \approx (\gamma_{1R}^2 + \gamma_{1L}^2)/2 - \gamma_{1L}\gamma_{1R} = 0$. Then

$$\begin{aligned} C_e(s) &= \frac{1}{s - \gamma_{1L}\gamma_{1R} e^{-2z_1 s/c} + \frac{\gamma_{1R}^2 + \gamma_{1L}^2}{2}} \\ &\approx \frac{1}{s - \gamma_{1L}\gamma_{1R} + \frac{\gamma_{1R}^2 + \gamma_{1L}^2}{2}} = \frac{1}{s}, \end{aligned} \quad (49)$$

and $\lim_{t \rightarrow \infty} c_e(t) = \lim_{s \rightarrow 0} sC_e(s) = 1$. □

In the above, we generalized the control performance that the atom is nonchirally coupled with the waveguide in (Bradford and Shen, 2013) to that the atom is chirally coupled with the waveguide. To compare with the result in (Bradford and Shen, 2013), where the mirror is at the right terminal of the waveguide, we first derive its counterpart when the mirror is at the left terminal of the waveguide. After that we compare the populations of the excited atomic state and the right propagating single-photon wave packet. The performances with $z_1 = 2.25\pi/\omega_a$ and $\omega_a = 50$ are given in Fig. 5, where (a) is for the population $|c_e(t)|^2$ and (b) is for the right-propagating photon wave packet solved in **Appendix C**. For the nonchiral coupling as in (Bradford and Shen, 2013), we take $\gamma_{1R} = \gamma_{1L} = 0.2$, while we let $\gamma_{1R} = 3\gamma_{1L} = 0.3$ and $\gamma_{1R} = 7\gamma_{1L} = 0.35$ for the chiral couplings respectively. Here for the simulations of the right-propagating photon wave packet, $g_r(t - z/c)$ is given by replacing t in the right hand side of Eq. (C.11) with $t - z/c$. The simulations that $\gamma_{1R} < \gamma_{1L}$ are similar with the circumstance that $\gamma_{1R} > \gamma_{1L}$.

Remark 5 In the parameters settings in Fig. 5, $e^{i2\omega_a z_1/c} = i$ and $\gamma_{1L} + \gamma_{1R} = 0.4$, $|c_e(t)|^2 = e^{-(\gamma_{1L}^2 + \gamma_{1R}^2)t} \leq e^{-(\gamma_{1L} + \gamma_{1R})^2 t/2}$ with the equality established only when $\gamma_{1L} = \gamma_{1R}$. Thus the chiral coupling can induce faster decaying of the excited atomic state.

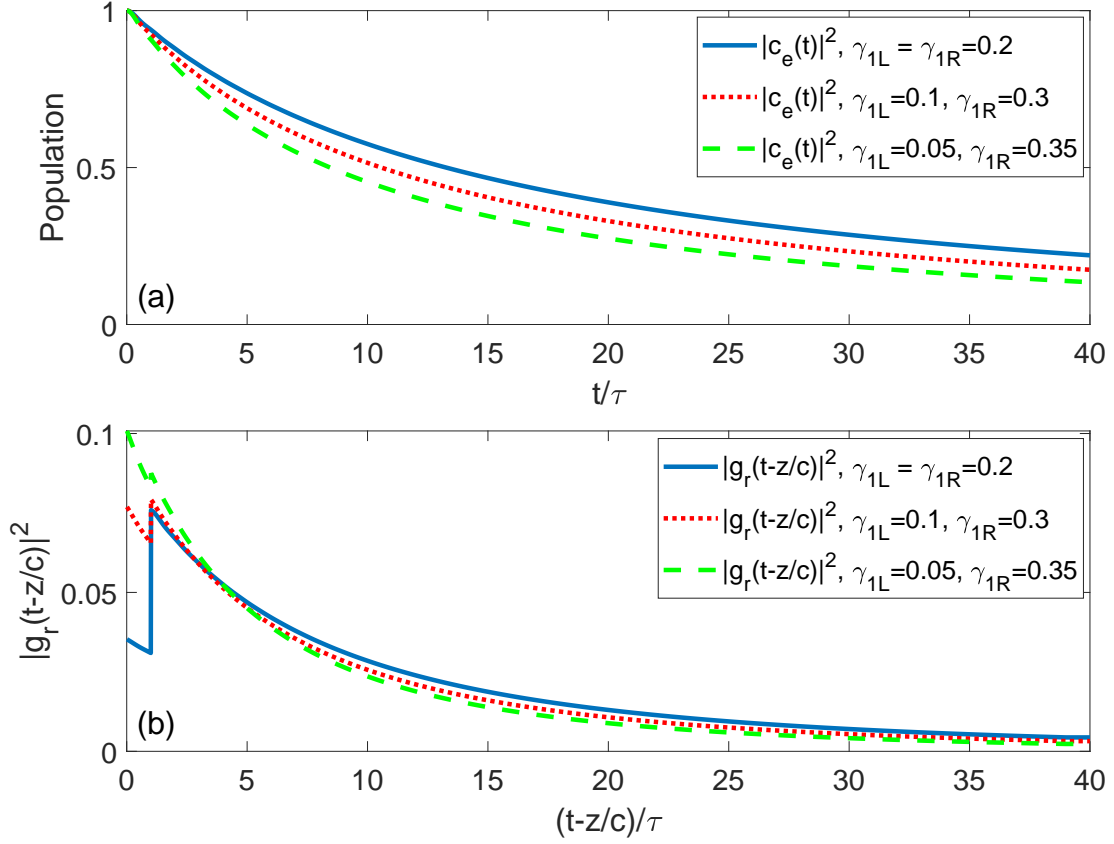


Figure 5: Comparison of the feedback control with chiral coupling and nonchiral coupling (in (Bradford and Shen, 2013)) between one atom and the semi-infinite waveguide.

The conclusion in **Theorem 8** agrees with the analysis in the frequency domain in (Tufarelli et al., 2013), which clarifies that at the exact parameter setting of the location of the first atom, there will not be any photons emitted into the waveguide and the atom functions as an atomic mirror. Considering that **Theorem 8** holds only when the interaction between the atom and the waveguide is nonchiral, this can also be derived from the nonchiral model in (Bradford and Shen, 2013).

3.1.1. The influence of the feedback loop length on stability

As studied in (Olbrot, 1984), when $\gamma_{1L} \neq \gamma_{1R}$ or $\cos(\omega_a \tau_1) < 1$, the delayed system (46) is asymptotically stable. However, when the delay τ_1 is large enough, the system may not be exponentially stable. To show this, we first rewrite the delay-dependent equation Eq. (46) as real-value equations in terms of the real and imaginary parts of $c_e(t)$, which is

$$\begin{cases} \dot{c}_e^R(t) = -\gamma_{RL}^{(1)} c_e^R(t) + \mathbf{g}_1 \left[c_e^R(t - \tau_1) \cos(\omega_a \tau_1) - c_e^I(t - \tau_1) \sin(\omega_a \tau_1) \right], \\ \dot{c}_e^I(t) = -\gamma_{RL}^{(1)} c_e^I(t) + \mathbf{g}_1 \left[c_e^R(t - \tau_1) \sin(\omega_a \tau_1) + c_e^I(t - \tau_1) \cos(\omega_a \tau_1) \right], \end{cases} \quad (50a)$$

$$\quad (50b)$$

where $c_e(t) = c_e^R(t) + ic_e^I(t)$, $\gamma_{RL}^{(1)} = (\gamma_{1R}^2 + \gamma_{1L}^2)/2$. Denote $\mathbf{x}_1(t) = [c_e^R(t), c_e^I(t)]^T$. Define $\tilde{A} = \begin{bmatrix} -\gamma_{RL}^{(1)} & 0 \\ 0 & -\gamma_{RL}^{(1)} \end{bmatrix}$,

$\tilde{B} = \mathbf{g}_1 \begin{bmatrix} \cos(\omega_a \tau_1) & -\sin(\omega_a \tau_1) \\ \sin(\omega_a \tau_1) & \cos(\omega_a \tau_1) \end{bmatrix}$. Then Eq. (50) becomes

$$\dot{\mathbf{x}}_1(t) = \tilde{A} \mathbf{x}_1(t) + \tilde{B} \mathbf{x}_1(t - \tau_1), \quad (51)$$

whose characteristic quasi-polynomial is

$$\begin{aligned} \Delta_1(s) &= |sI - \tilde{A} - \tilde{B}e^{-\tau_1 s}| \\ &= \begin{vmatrix} s + \gamma_{RL}^{(1)} - \mathbf{g}_1 \cos(\omega_a \tau_1) e^{-\tau_1 s} & \mathbf{g}_1 \sin(\omega_a \tau_1) e^{-\tau_1 s} \\ -\mathbf{g}_1 \sin(\omega_a \tau_1) e^{-\tau_1 s} & s + \gamma_{RL}^{(1)} - \mathbf{g}_1 \cos(\omega_a \tau_1) e^{-\tau_1 s} \end{vmatrix} \\ &= (s + \gamma_{RL}^{(1)} - \mathbf{g}_1 \cos(\omega_a \tau_1) e^{-\tau_1 s})^2 + (\mathbf{g}_1 \sin(\omega_a \tau_1) e^{-\tau_1 s})^2 \\ &= (s + \gamma_{RL}^{(1)})^2 - 2\mathbf{g}_1 \cos(\omega_a \tau_1) (s + \gamma_{RL}^{(1)}) e^{-\tau_1 s} + \mathbf{g}_1^2 e^{-2\tau_1 s}. \end{aligned} \quad (52)$$

Next, we consider the circumstance that τ_1 is large enough. We denote the solutions of $\Delta_1(s) = 0$ as \tilde{s} for convenience.

Theorem 9 *For arbitrary $\epsilon > 0$, there exists $\tau_1 > \tau_\epsilon > 0$, such that there is one root of Eq. (52) which satisfies that $\text{Re}(\tilde{s}) \geq -\epsilon$ and therefore the atomic steady state is not the ground state.*

Proof *The proof of $\text{Re}(\tilde{s}) \geq -\epsilon$ is similar to that of Theorem 1 in (Olbro, 1984), thus is omitted. This, together with that there are no oscillating behavior as determined by the Lindblad master equation (33), the steady value of $c_e(t)$ can be nonzero, which means the atomic steady state is not the ground state.*

Based on **Theorem 9**, the influence of atomic dynamics by delays is further illustrated in the following simulations. In Fig. 6, one two-level atom is coupled with the semi-infinite waveguide at z_1 . Parameters are $\omega_a = 50$, $\gamma_{1L} = 0.2$ and $\gamma_{1R} = 0.6$ in (a), and $\gamma_{1L} = \gamma_{1R} = 0.2$ in (b). As shown in the chiral parameter setting in (a), an initially excited atom certainly decays to the ground state. Moreover, the decaying rate is much smaller when $z_1 = n\pi/\omega_a$ with $n = 1, 2, \dots$, which agrees with Eq. (48), **Theorem 8**, or the simplified **Theorem 1**. On the other hand, in the nonchiral parameter setting in (b), the large delay can induce non-zero steady excited populations, which agrees with the conclusion in **Theorem 9**.

Remark 6 *When the atom is far from the terminal mirror of the semi-infinite waveguide, the emitted filed by the atom to the mirror can re-excite the atom after being reflected, resulting in the non-zero populations of the atomic states. This means that the non-Markovian quantum dynamics realized by a coherent feedback channel can make a difference compared with the Markovian circumstance with a short delay.*

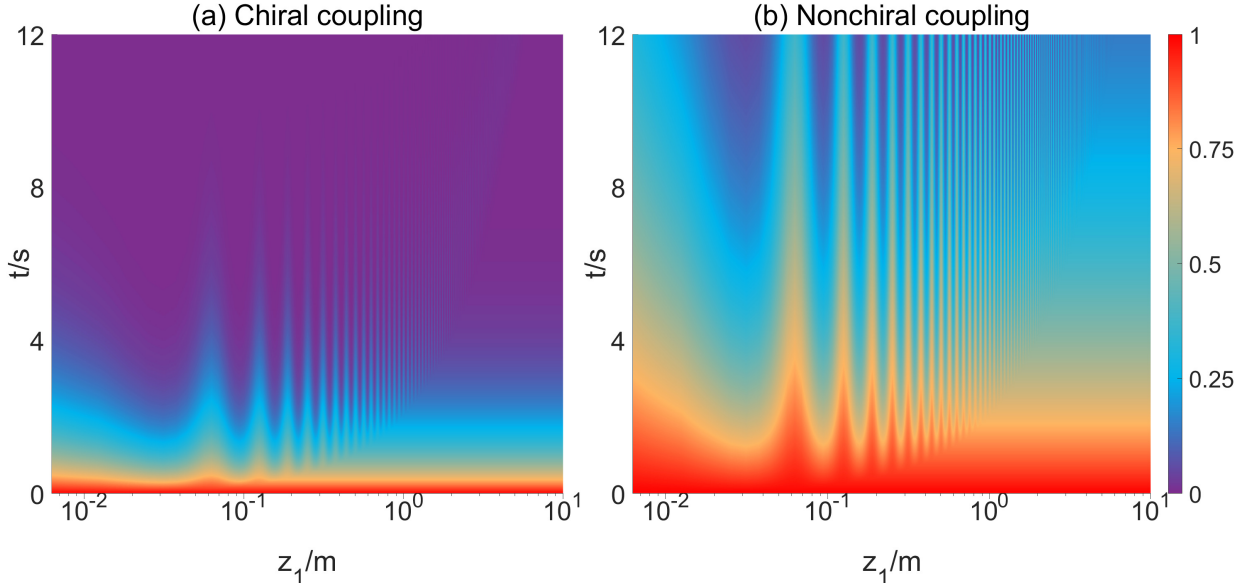


Figure 6: Atom populations influenced by delay.

3.2. The two-atoms dynamics in the spatial domain

In this subsection, we analyze in the spatial domain the dynamics that two atoms are coupled with a semi-infinite waveguide.

When there are two atoms coupled with the semi-infinite waveguide, the Hamiltonian for the two-atom case, as the counterpart of that in Eq.(43) for the single-atom case, reads

$$H = \sum_{j=1,2} (\hbar\tilde{\omega}_1|g_j\rangle\langle g_j| + \hbar\tilde{\omega}_2|e_j\rangle\langle e_j|) + H_w + H_m + \sum_{j=1,2} H_1^{(j)}, \quad (53)$$

where H_w and H_m are given in Eq. (43), and $H_1^{(j)}$ is generalized from Eq. (B.5) as

$$H_1^{(j)} = -i \int_{-\infty}^{\infty} [\gamma_{jRCR}(z)\delta(z - z_j) + \gamma_{jLCL}(z)\delta(z - z_j)] \sigma_j^+ dz + \text{H.c.}, \quad (54)$$

where $j = 1, 2$.

We assume initially only the first atom is excited, and there can be at most one photon in the waveguide. Then the quantum state can be represented as

$$\begin{aligned} |\Psi(t)\rangle &= \sum_{j=1,2} c_j(t) e^{-i(\tilde{\omega}_1 + \tilde{\omega}_2)t} \sigma_j^+ |g_1, g_2, \{0\}\rangle \\ &+ \int_0^{\infty} \Phi_g^l(t, z) e^{-i2\tilde{\omega}_1 t} |g_1, g_2, 1_z^r\rangle dz + \int_0^{\infty} \Phi_g^l(t, z) e^{-i2\tilde{\omega}_1 t} |g_1, g_2, 1_z^l\rangle dz, \end{aligned} \quad (55)$$

where $c_j(t)$ represents the amplitude that the j th atom is excited and there is not any photons in the waveguide, $\Phi_g^r(t, z)$ and $\Phi_g^l(t, z)$ represent the amplitudes of the states that both of the two atoms are in the ground state and there is one

right or left-propagating photon in the waveguide respectively. Take the state representation into the Schrödinger equation and we have

$$\left\{ \begin{array}{l} \dot{c}_j(t) = -\gamma_{jR}\Phi_g^r(t, z_j)e^{i\omega_a t} - \gamma_{jL}\Phi_g^l(t, z_j)e^{i\omega_a t}, \\ \frac{\partial \Phi_g^r(t, z)}{\partial t} = -v_g \frac{\partial \Phi_g^r(t, z)}{\partial z} + 2v_g \Phi_g^l(t, z)e^{2ikz}\delta(z) \\ \quad + \sum_{j=1,2} \gamma_{jR}c_j(t)\delta(z - z_j)e^{-i\omega_a t}, \\ \frac{\partial \Phi_g^l(t, z)}{\partial t} = v_g \frac{\partial \Phi_g^l(t, z)}{\partial z} - 2v_g \Phi_g^r(t, z)e^{-2ikz}\delta(z) \\ \quad + \sum_{j=1,2} \gamma_{jL}c_j(t)\delta(z - z_j)e^{-i\omega_a t}. \end{array} \right. \quad (56a)$$

$$\quad (56b)$$

$$\quad (56c)$$

Then $\Phi_g^r(t, z)$ and $\Phi_g^l(t, z)$ can be further represented as

$$\left\{ \begin{array}{l} \Phi_g^r(z, t) = [\Theta(z) - \Theta(z - z_1)] f_r(t - z/c) \\ \quad + [\Theta(z - z_1) - \Theta(z - z_2)] g_r(t - z/c) \\ \quad + \Theta(z - z_2) h_r(t - z/c), \\ \Phi_g^l(z, t) = [\Theta(z) - \Theta(z - z_1)] f_l(t + z/c) \\ \quad + [\Theta(z - z_1) - \Theta(z - z_2)] g_l(t + z/c), \end{array} \right. \quad (57a)$$

$$\quad (57b)$$

where $f_r(t - z/c)$, $g_r(t - z/c)$ and $h_r(t - z/c)$ represent the right-propagating photon wave packets at $[0, z_1]$, $[z_1, z_2]$ and $[z_2, +\infty]$, $f_l(t + z/c)$ and $g_l(t + z/c)$ are for the left-propagating photon wave packets at $[0, z_1]$ and $[z_1, z_2]$, respectively.

Furthermore, $c_j(t)$ with $j = 1, 2$ can be solved in the spatial domain as illustrated in **Appendix D**, which agrees with the analysis in the frequency domain in (Zhang et al., 2020). While the spatial distribution of the photon wave packet can be clarified based on Eq. (56) and solved as Eq. (D.7), which cannot be covered in the frequency domain analysis. As compared in Fig. 7 (a) with $z_2 = 10z_1 = 10$ and $\omega_a = 50$, the first atom decays via the spontaneous emission, and the emitted photon can further excite the second atom after the direct transmission or the reflection by the mirror. As a result, the second atom can be transiently more excited by the right-propagating photon wave packet emitted by the first atom, especially when γ_{2R} is much larger than γ_{2L} . The right propagating photon wave packets at $z > z_2$ are compared in Fig. 7 (b) by combining Eqs. (D.7c,D.7d,D.7e), which is influenced by the locations of the atoms and the reflection of the mirror.

Remark 7 *The advantage of the spatial domain analysis is that the spatial distribution and propagation of the photon wavepacket can be manifested, which cannot be solved by modeling in the frequency domain. However, the atom population dynamics in the spatial domain must be equivalent with the format in the frequency domain, as in (Zhang et al., 2020; Huo and Li, 2020; Guimond et al., 2017; Pichler and Zoller, 2016).*

3.3. Spontaneous emission rate in the spatial domain

On one hand, when one atom is coupled with the waveguide, as given in Eq. (46), the atom's spontaneous emission rate is $(\gamma_{1R}^2 + \gamma_{1L}^2)/2v_g$, which agree with the result by in the frequency domain as in **Section 2**. This can also be

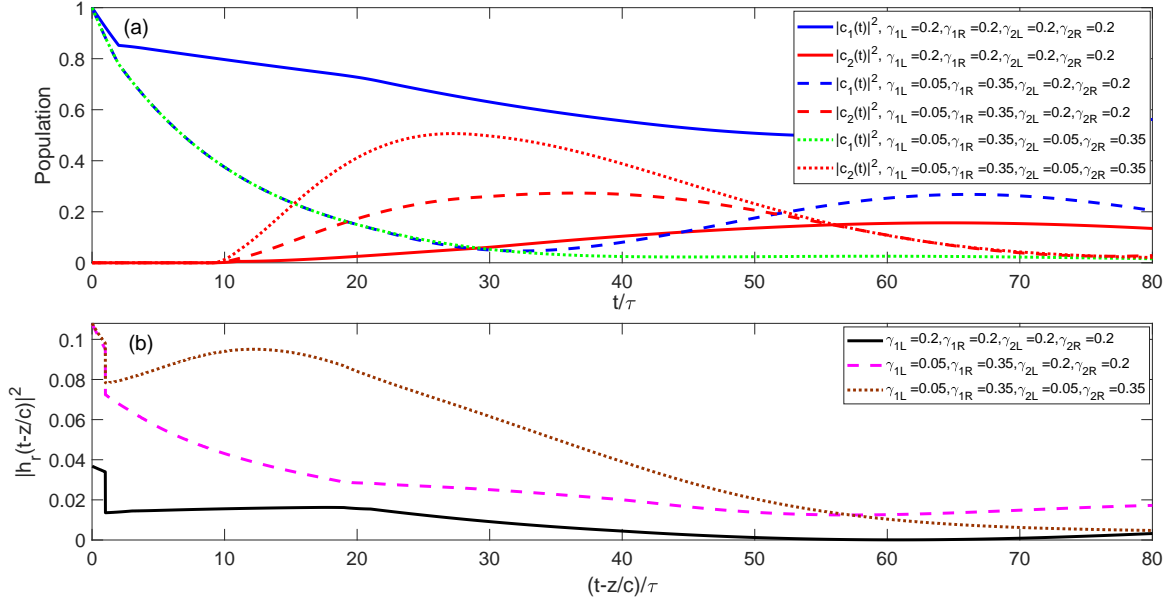


Figure 7: Comparison of the feedback control of two atoms with one excitation.

generalized to the two-atom case in the spatial domain as in Eq. (D.3) and Eq. (D.6).

On the other hand, the emission rate of photons can also be studied in the spatial domain as given in Eqs. (C.9,C.11) for the one-atom case and Eq. (D.7) for the two-atom case, respectively. It can be seen from Eq. (D.7) that the photon emission rate towards mirror (left-propagating modes) in the wave-guide and one leaving the system (right-propagating modes) are determined by the chiral couplings and atom locations.

3.4. Non-exponentially stable dynamics induced by large coherent feedback delays

When there are two atoms coupled with the semi-infinite waveguide, and initially only the first atom is excited, Eq. (56a) can be equivalently written in a delay dependent format as (Guimond et al., 2017; Zhang et al., 2020; Pichler and Zoller, 2016)

$$\begin{cases} \dot{c}_1(t) = -\frac{\gamma_{1R}^2 + \gamma_{1L}^2}{2} c_1(t) - \gamma_{1L}\gamma_{2L}c_2\left(t - \frac{z_2 - z_1}{c}\right) e^{i\omega_a \frac{z_2 - z_1}{c}} \\ \quad + \gamma_{1R}\gamma_{1L}c_1\left(t - \frac{2z_1}{c}\right) e^{i\omega_a \frac{2z_1}{c}} + \gamma_{1R}\gamma_{2L}c_2\left(t - \frac{z_1 + z_2}{c}\right) e^{i\omega_a \frac{z_1 + z_2}{c}}, \\ \dot{c}_2(t) = -\frac{\gamma_{2R}^2 + \gamma_{2L}^2}{2} c_2(t) - \gamma_{2R}\gamma_{1R}c_1\left(t - \frac{z_2 - z_1}{c}\right) e^{i\omega_a \frac{z_2 - z_1}{c}} \\ \quad + \gamma_{2R}\gamma_{2L}c_2\left(t - \frac{2z_2}{c}\right) e^{i\omega_a \frac{2z_2}{c}} + \gamma_{2R}\gamma_{1L}c_1\left(t - \frac{z_1 + z_2}{c}\right) e^{i\omega_a \frac{z_1 + z_2}{c}}, \end{cases} \quad (58a)$$

$$\begin{cases} \dot{c}_1(t) = -\frac{\gamma_{1R}^2 + \gamma_{1L}^2}{2} c_1(t) - \gamma_{1L}\gamma_{2L}c_2\left(t - \frac{z_2 - z_1}{c}\right) e^{i\omega_a \frac{z_2 - z_1}{c}} \\ \quad + \gamma_{1R}\gamma_{1L}c_1\left(t - \frac{2z_1}{c}\right) e^{i\omega_a \frac{2z_1}{c}} + \gamma_{1R}\gamma_{2L}c_2\left(t - \frac{z_1 + z_2}{c}\right) e^{i\omega_a \frac{z_1 + z_2}{c}}, \\ \dot{c}_2(t) = -\frac{\gamma_{2R}^2 + \gamma_{2L}^2}{2} c_2(t) - \gamma_{2R}\gamma_{1R}c_1\left(t - \frac{z_2 - z_1}{c}\right) e^{i\omega_a \frac{z_2 - z_1}{c}} \\ \quad + \gamma_{2R}\gamma_{2L}c_2\left(t - \frac{2z_2}{c}\right) e^{i\omega_a \frac{2z_2}{c}} + \gamma_{2R}\gamma_{1L}c_1\left(t - \frac{z_1 + z_2}{c}\right) e^{i\omega_a \frac{z_1 + z_2}{c}}, \end{cases} \quad (58b)$$

as derived in the spatial domain in **Appendix D** or in the frequency domain (Zhang et al., 2020). The dynamics when z_1 and z_2 are small has been studied by (Zhang et al., 2020). Now, we study the non-exponential stability dynamics when the delay is relative large.

Theorem 10 When $z_1 \lesssim z_2 = n\pi/\omega_a$ for some integer $n \gg 1$ and $\tau_1 \gg 0$, $\gamma_{1R} = \gamma_{1L} = \gamma_1$, $\gamma_{2R} = \gamma_{2L} = \gamma_2$, the two atoms have non-zero steady population satisfying $|c_1/c_2| = \gamma_1/\gamma_2$.

Proof In this parameter setting, the evolution of the atomic amplitudes read

$$\begin{bmatrix} \dot{c}_1(t) \\ \dot{c}_2(t) \end{bmatrix} = \begin{bmatrix} -\gamma_1^2 & -\gamma_1\gamma_2 \\ -\gamma_1\gamma_2 & -\gamma_2^2 \end{bmatrix} \begin{bmatrix} c_1(t) \\ c_2(t) \end{bmatrix} + e^{i\omega_a\tau_1} \begin{bmatrix} \gamma_1^2 & \gamma_1\gamma_2 \\ \gamma_1\gamma_2 & \gamma_2^2 \end{bmatrix} \begin{bmatrix} c_1(t - \tau_1) \\ c_2(t - \tau_1) \end{bmatrix}. \quad (59)$$

When $n \gg 1$, $c_1(t)$ and $c_2(t)$ can be solved using the method introduced in the proof of Theorem 1 in (Ding et al., 2023), thus is omitted here. When n and τ_1 are large, $c_1(\tau_1) \approx \frac{\gamma_1^2}{\gamma_1^2 + \gamma_2^2}$, and $c_2(\tau_1) \approx -\frac{\gamma_1\gamma_2}{\gamma_1^2 + \gamma_2^2}$. When $t > t_1$, according to the the proof of Theorem 1 of (Ding et al., 2023), $c_1(t)$ and $c_2(t)$ are asymptotically stable around $c_1(\tau_1)$ and $c_2(\tau_1)$ respectively.

Remark 8 *Theorem 10* means that when the delay in the waveguide-atom network is large, and the coupling between the atom and waveguide is nonchiral, the atomic state can be non-exponentially stable and have non-zero steady values. A simplified example is the one-atom case in Fig. 6(b), where the atom does not settle to the ground state when z_1 is large.

3.5. Comparison with cavity-QED system

In this section, we compare the stability and steady states of the coherent feedback network in Fig. 1 and other coherent feedback network schemes based on cavity-QED systems. For simplicity, we only consider the case where there is one two-level atom in resonance with the cavity in the coherent feedback network, which has been studied in (Német et al., 2019; Ding and Zhang, 2023; Crowder et al., 2020). The cavity QED system can be represented with the Jaynes-Cummings model

$$H_{\text{JC}} = -g_c (a\sigma_1^+ + a^\dagger\sigma_1^-), \quad (60)$$

where a (a^\dagger) is the annihilation(creation) operator for the cavity, and g_c is the coupling strength between the atom and cavity. When the coherent feedback is realized by the cavity QED system coupled with a round-trip waveguide, the interaction Hamiltonian can be generalized from Eq. (4) to (Ding and Zhang, 2023; Német et al., 2019; Crowder et al., 2020)

$$H_{\text{I}}^{C-W} = H_{\text{JC}} + \int [g_{k1t}(k, t, z)d_k^\dagger a + g_{k1t}^*(k, t, z)d_k a^\dagger] dk, \quad (61)$$

with $d_k^\dagger a$ and $d_k a^\dagger$ representing the coupling or exchanging of photons between the waveguide and cavity.

On the other hand, when the coherent feedback loop for the cavity QED system is closed by another cavity as (Lang et al., 1973; Gea-Banacloche et al., 1990; Gea-Banacloche, 2013; Német et al., 2019) or Section III of (Ding and Zhang, 2023), the interaction Hamiltonian for the coherent feedback network reads (Német et al., 2019; Ding and Zhang, 2023)

$$H_{\text{I}}^{C-C} = H_{\text{JC}} + \sum_k \left[g_{k1t} \left(\frac{\omega_k}{c}, t, z \right) d_k^\dagger a + g_{k1t}^* \left(\frac{\omega_k}{c}, t, z \right) d_k a^\dagger \right], \quad (62)$$

where the cavity for feedback can be modeled in analog with a waveguide with discrete modes (Lang et al., 1973; Német et al., 2019; Ding and Zhang, 2023). We compare the atomic dynamics evaluated by $c_{e1}(t)$ in Eq. (17) as follows.

Lemma 1 (Ding and Zhang, 2023; Német et al., 2019) *For the coherent feedback network in Eq. (61), $c_{e1}(t)$ is exponentially stable when $z_1 \neq n\pi/\omega_a \ll c$, and is oscillating when $z_1 = n\pi/\omega_a \ll c$ for some integer n .*

Lemma 2 (Ding and Zhang, 2023) *For the coherent feedback network in Eq. (62), $c_{e1}(t)$ is always oscillating for arbitrary z_1 .*

In the following, we compare the coherent feedback dynamics based on waveguide QED and cavity QED systems.

Theorem 11 *The coherent feedback network by a round-trip waveguide with continuous modes can induce exponentially decaying atomic states or persistently excited steady state, while can induce exponentially decaying states or oscillating states for a Jaynes-Cummings model without persistently excited atomic state.*

Proof *The first half of the statement can be proved by combining **Theorems 1-10**, and the second half of the statement can be proved by combining **Lemma 1** and **Lemma 2**.*

Remark 9 *The coherent feedback for a cavity QED (in Eqs. (61,62)) cannot induce persistently excited atomic state, but only oscillating atomic states when the photon in the cavity and cannot be emitted into the waveguide.*

The above comparisons illustrate that the coherent feedback loop realized by a waveguide makes it possible for the generation of stable photonic states via the spontaneous emission of atoms. When the atom is directly coupled with the waveguide instead of via a cavity, the atom can be persistently excited with non-zero steady excited populations, which will never occur when the atom is in a cavity.

4. Conclusion

In this paper, we have studied the coherent feedback control dynamics based on atom-waveguide interactions with multiple delays induced by the transportation of photons in the waveguide. When the atoms are initially excited, the number of generated photons in the waveguide is influenced by the locations of the atoms and their chiral coupling strengths with different directional propagating modes in the waveguide. When the locations of the atoms and their chiral coupling strengths with the waveguide are properly designed, two-photon, one-photon and zero-photon states can be generated in the waveguide. The quantum coherent feedback control based on waveguide QED can be analyzed from the perspective of linear system control with delays, and large delays can induce excited steady atomic states, which is different from the case that the coherent feedback delays are small. Moreover, the spatial modeling of this quantum system provides another approach to investigating the coherent feedback dynamics, and the examples of the

one-atom and two-atom cases have provided a comprehensive study when combining the spatial domain modeling with the frequency domain modeling.

Appendix

Appendix A. Derivations of Eqs. (9,10,11)

In this appendix, we derive Eqs. (9,10,11) in the main text, which demonstrate clearly the influence of the round-trip delays on the dynamics of the coherent feedback network in Fig. 1.

(1) Derivation of Eq. (10).

For the second component on the right-hand side of Eq. (8b), $c_{kk}(k, k_1, t)$ can be replaced with the integration of Eq. (8d); specifically,

$$\begin{aligned}
& -i \int c_{kk}(k, k_1, t) g_{k1t}^*(k_1, t, z_1) dk_1 \\
= & - \int_0^t du \int [c_{egk}(u, k) g_{k1t}(k_1, u, z_1) + c_{egk}(u, k_1) g_{k1t}(k, u, z_1) \\
& + c_{gek}(u, k) g_{k2t}(k_1, u, z_2) + c_{gek}(u, k_1) g_{k2t}(k, u, z_2)] g_{k1t}^*(k_1, t, z_1) dk_1.
\end{aligned} \tag{A.1}$$

Noticing that

$$\begin{aligned}
& \int c_{egk}(u, k) g_{k1t}(k_1, u, z_1) g_{k1t}^*(k_1, t, z_1) dk_1 \\
= & \int c_{egk}(u, k) [\gamma_{1R}^2 e^{i(\omega_1 - \omega_a)(u-t)} + \gamma_{1L}^2 e^{i(\omega_1 - \omega_a)(u-t)} \\
& - \gamma_{1L}\gamma_{1R} e^{i[(\omega_1 - \omega_a)(u-t) + 2\omega_1 z_1/c]} - \gamma_{1R}\gamma_{1L} e^{i[(\omega_1 - \omega_a)(u-t) - 2\omega_1 z_1/c]}] dk_1 \\
= & \int c_{egk}(u, k) e^{-i\omega_a(u-t)} [\gamma_{1R}^2 e^{i\omega_1(u-t)} + \gamma_{1L}^2 e^{i\omega_1(u-t)} \\
& - \gamma_{1L}\gamma_{1R} e^{i\omega_1(u-t+2z_1/c)} - \gamma_{1R}\gamma_{1L} e^{i\omega_1(u-t-2z_1/c)}] dk_1 \\
= & c_{egk}(u, k) e^{-i\omega_a(u-t)} [\gamma_{1R}^2 \delta(u-t) + \gamma_{1L}^2 \delta(u-t) \\
& - \gamma_{1L}\gamma_{1R} \delta(u-t+2z_1/c) - \gamma_{1R}\gamma_{1L} \delta(u-t-2z_1/c)],
\end{aligned} \tag{A.2}$$

thus the first component in Eq. (A.1) becomes

$$\begin{aligned}
& \int_0^t du \int c_{egk}(u, k) g_{k1t}(k_1, u, z_1) g_{k1t}^*(k_1, t, z_1) dk_1 \\
= & \int_0^t du c_{egk}(u, k) e^{-i\omega_a(u-t)} [\gamma_{1R}^2 \delta(u-t) + \gamma_{1L}^2 \delta(u-t) \\
& - \gamma_{1L}\gamma_{1R} \delta(u-t+2z_1/c) - \gamma_{1R}\gamma_{1L} \delta(u-t-2z_1/c)] \\
= & \frac{\gamma_{1R}^2 + \gamma_{1L}^2}{2} c_{egk}(t, k) - \gamma_{1L}\gamma_{1R} c_{egk}(t-2z_1/c, k) e^{i\omega_a \frac{2z_1}{c}},
\end{aligned} \tag{A.3}$$

which means that the temporal evolution of $c_{egk}(t, k)$ is influenced not only by the chiral coupling strengths, but also by the round-trip delay between the first atom and the mirror.

For the second component in Eq. (A.1), we have

$$\begin{aligned}
& \int c_{egk}(u, k_1) g_{k1t}(k, u, z_1) g_{k1t}^*(k_1, t, z_1) dk_1 \\
&= \int c_{egk}(u, k_1) \left\{ i\gamma_{1R} e^{i[(\omega - \omega_a)u - \omega z_1/c]} - i\gamma_{1L} e^{i[(\omega - \omega_a)u + \omega z_1/c]} \right. \\
&\quad \left. \left\{ -i\gamma_{1R} e^{-i[(\omega_1 - \omega_a)t - \omega_1 z_1/c]} + i\gamma_{1L} e^{-i[(\omega_1 - \omega_a)t + \omega_1 z_1/c]} \right\} dk_1, \right.
\end{aligned} \tag{A.4}$$

which equals zero according to the following lemma.

Lemma 3 For the finite amplitude $c_{egk}(u, k_1)$ which is a continuous function of the time variable u , we have

$$\int c_{egk}(u, k_1) e^{-i[(\omega_1 - \omega_a)t - \omega_1 z_1/c]} dk_1 = 0.$$

Proof Notice that

$$\begin{aligned}
& \int c_{egk}(u, k_1) e^{-i[(\omega_1 - \omega_a)t - \omega_1 z_1/c]} dk_1 \\
&= e^{i\omega_a t} \int c_{egk}(u, k_1) e^{-i\omega_1(t - z_1/c)} dk_1 \\
&= e^{i\omega_a t} \left[\int e^{-i\omega_1(t - z_1/c)} dk_1 c_{egk}(u, k_1) - \int \int e^{-i\omega_1'(t - z_1/c)} dk_1' \frac{dc_{egk}(u, k_1)}{dk_1} dk_1 \right] \\
&= e^{i\omega_a t} \left[\delta(t - z_1/c) c_{egk}(u, k_1) - \int \delta(t - z_1/c) \frac{dc_{egk}(u, k_1)}{dk_1} dk_1 \right].
\end{aligned} \tag{A.5}$$

When $t \neq z_1/c$, $\delta(t - z_1/c) = 0$, consequently $\int c_{egk}(u, k_1) e^{-i[(\omega_1 - \omega_a)t - \omega_1 z_1/c]} dk_1 = 0$. Because c_{egk} is continuous, $\int c_{egk}(u, k_1) e^{-i[(\omega_1 - \omega_a)t - \omega_1 z_1/c]} dk_1 = 0$ for arbitrary u . \square

For the third component of Eq. (A.1), the integration with respect to k_1 yields

$$\begin{aligned}
& \int c_{gek}(u, k) g_{k2t}(k_1, u, z_2) g_{k1t}^*(k_1, t, z_1) dk_1 \\
&= c_{gek}(u, k) \int \left\{ \gamma_{1R}\gamma_{2R} e^{i[(\omega_1 - \omega_a)(u-t) - \omega_1(z_2 - z_1)/c]} - \gamma_{1R}\gamma_{2L} e^{i[(\omega_1 - \omega_a)(u-t) + \omega_1(z_1 + z_2)/c]} \right. \\
&\quad \left. - \gamma_{2R}\gamma_{1L} e^{i[(\omega_1 - \omega_a)(u-t) - \omega_1(z_2 + z_1)/c]} + \gamma_{1L}\gamma_{2L} e^{i[(\omega_1 - \omega_a)(u-t) + \omega_1(z_2 - z_1)/c]} \right\} dk_1 \\
&= c_{gek}(u, k) e^{-i\omega_a(u-t)} \int \left\{ \gamma_{1R}\gamma_{2R} e^{i\omega_1[u-t - (z_2 - z_1)/c]} - \gamma_{1R}\gamma_{2L} e^{i\omega_1[u-t + (z_1 + z_2)/c]} \right. \\
&\quad \left. - \gamma_{2R}\gamma_{1L} e^{i\omega_1[u-t - (z_2 + z_1)/c]} + \gamma_{1L}\gamma_{2L} e^{i\omega_1[u-t + (z_2 - z_1)/c]} \right\} dk_1 \\
&= c_{gek}(u, k) e^{-i\omega_a(u-t)} \left[\gamma_{1R}\gamma_{2R} \delta\left(u - t - \frac{z_2 - z_1}{c}\right) - \gamma_{1R}\gamma_{2L} \delta\left(u - t + \frac{z_1 + z_2}{c}\right) \right. \\
&\quad \left. - \gamma_{2R}\gamma_{1L} \delta\left(u - t - \frac{z_2 + z_1}{c}\right) + \gamma_{1L}\gamma_{2L} \delta\left(u - t + \frac{z_2 - z_1}{c}\right) \right].
\end{aligned} \tag{A.6}$$

As a result, the third component of Eq. (A.1) reads

$$\begin{aligned}
& \int_0^t \int c_{gek}(u, k) g_{k2t}(k_1, u, z_2) g_{k1t}^*(k_1, t, z_1) dk_1 du \\
&= \int_0^t c_{gek}(u, k) e^{-i\omega_a(u-t)} \left[-\gamma_{1R}\gamma_{2L} \delta\left(u - t + \frac{z_1 + z_2}{c}\right) + \gamma_{1L}\gamma_{2L} \delta\left(u - t + \frac{z_2 - z_1}{c}\right) \right] du \\
&= -\gamma_{1R}\gamma_{2L} c_{gek}\left(t - \frac{z_1 + z_2}{c}, k\right) e^{i\omega_a \frac{z_1 + z_2}{c}} + \gamma_{1L}\gamma_{2L} c_{gek}\left(t - \frac{z_2 - z_1}{c}, k\right) e^{i\omega_a \frac{z_2 - z_1}{c}}.
\end{aligned} \tag{A.7}$$

Clearly, the first term in Eq. (A.7) is related to the delay $(z_1 + z_2)/c$ induced when a left-propagating field is emitted by the second atom, and which is reflected by the mirror and interacts with the first atom, while the second term is related with the transmission delay $(z_2 - z_1)/c$ from the second atom to the first atom.

Similar to the proof for **Lemma 3**, it can be shown that

$$\int c_{gek}(u, k_1)g_{k2t}(k, u, z_2)g_{k1t}^*(k_1, t, z_1)dk_1 = 0.$$

Thus, the fourth component of Eq. (A.1) equals zero.

In summary, the evolution of $c_{gek}(t, k)$ can be rewritten as

$$\begin{aligned} \dot{c}_{gek}(t, k) = & -ic_{ee}(t)g_{k2t}(k, t, z_2) - \frac{\gamma_{1R}^2 + \gamma_{1L}^2}{2}c_{gek}(t, k) + \gamma_{1L}\gamma_{1R}c_{gek}(t - 2z_1/c, k)e^{i\omega_a \frac{2z_1}{c}} \\ & + \gamma_{1R}\gamma_{2L}c_{gek}\left(t - \frac{z_1 + z_2}{c}, k\right)e^{i\omega_a \frac{z_1 + z_2}{c}} - \gamma_{1L}\gamma_{2L}c_{gek}\left(t - \frac{z_2 - z_1}{c}, k\right)e^{i\omega_a \frac{z_2 - z_1}{c}}, \end{aligned} \quad (\text{A.8})$$

which is Eq. (10) in the main text.

(2) Derivation of Eq. (11).

The derivation of Eq. (11) is similar with that of Eq. (10), thus is omitted.

(3) Derivation of Eq. (9).

Take the integration of Eq. (A.8) into the first item on the right-hand side of Eq. (8a) yields

$$\begin{aligned} & \int c_{gek}(t, k)g_{k2t}^*(k, t, z_2)dk \\ = & \int \int_0^t \left\{ -ic_{ee}(u)g_{k2t}(k, u, z_2) - \frac{\gamma_{1R}^2 + \gamma_{1L}^2}{2}c_{gek}(u, k) \right. \\ & + \gamma_{1L}\gamma_{1R}c_{gek}(u - 2z_1/c, k)e^{i\omega_a \frac{2z_1}{c}} + \gamma_{1R}\gamma_{2L}c_{gek}\left(u - \frac{z_1 + z_2}{c}, k\right)e^{i\omega_a \frac{z_1 + z_2}{c}} \\ & \left. - \gamma_{1L}\gamma_{2L}c_{gek}\left(u - \frac{z_2 - z_1}{c}, k\right)e^{i\omega_a \frac{z_2 - z_1}{c}} \right\} g_{k2t}^*(k, t, z_2)du dk. \end{aligned} \quad (\text{A.9})$$

It is easy to show that the first inner integral

$$\begin{aligned} & -i \int \int_0^t c_{ee}(u)g_{k2t}(k, u, z_2)g_{k2t}^*(k, t, z_2)du dk \\ = & -i \int_0^t c_{ee}(u)e^{-i\omega_a(u-t)} \int \left[\gamma_{2R}^2 e^{i\omega(u-t)} \right. \\ & \left. - \gamma_{2L}\gamma_{2R}e^{i\omega(u-t+\frac{2z_2}{c})} - \gamma_{2L}\gamma_{2R}e^{i\omega(u-t-\frac{2z_2}{c})} + \gamma_{2L}^2 e^{i\omega(u-t)} \right] dk du \\ = & -i \int_0^t c_{ee}(u)e^{-i\omega_a(u-t)} \left[(\gamma_{2R}^2 + \gamma_{2L}^2) \delta(u-t) \right. \\ & \left. - \gamma_{2L}\gamma_{2R} \delta\left(u-t + \frac{2z_2}{c}\right) - \gamma_{2L}\gamma_{2R} \delta\left(u-t - \frac{2z_2}{c}\right) \right] du, \end{aligned} \quad (\text{A.10})$$

and the other inner integrals in Eq. (A.9) are all equal to zero according to **Lemma 3**. Thus

$$\int c_{gek}(t, k)g_{k2t}^*(k, t, z_2)dk = -i \frac{\gamma_{2R}^2 + \gamma_{2L}^2}{2} c_{ee}(t) + i\gamma_{2L}\gamma_{2R}c_{ee}\left(t - \frac{2z_2}{c}\right) e^{i\omega_a \frac{2z_2}{c}}. \quad (\text{A.11})$$

Similarly, for the second item on the right-hand side Eq. (8a), we have

$$\begin{aligned} & \int c_{gek}(t, k) g_{k1t}^*(k, t, z_1) dk \\ &= -i \left[\frac{\gamma_{1R}^2 + \gamma_{1L}^2}{2} c_{ee}(t) - \gamma_{1L} \gamma_{1R} c_{ee} \left(t - \frac{2z_1}{c} \right) e^{i\omega_a \frac{2z_1}{c}} \right]. \end{aligned} \quad (\text{A.12})$$

Therefore, the evolution of $c_{ee}(t)$ can be written as

$$\begin{aligned} & \dot{c}_{ee}(t) \\ &= -i \left[-i \frac{\gamma_{2R}^2 + \gamma_{2L}^2}{2} c_{ee}(t) + i \gamma_{2L} \gamma_{2R} c_{ee} \left(t - \frac{2z_2}{c} \right) e^{i\omega_a \frac{2z_2}{c}} \right] \\ & \quad - \left[\frac{\gamma_{1R}^2 + \gamma_{1L}^2}{2} c_{ee}(t) - \gamma_{1L} \gamma_{1R} c_{ee} \left(t - \frac{2z_1}{c} \right) e^{i\omega_a \frac{2z_1}{c}} \right] \\ &= -\frac{\gamma_{1R}^2 + \gamma_{1L}^2 + \gamma_{2R}^2 + \gamma_{2L}^2}{2} c_{ee}(t) \\ & \quad + \gamma_{1L} \gamma_{1R} c_{ee} \left(t - \frac{2z_1}{c} \right) e^{i\omega_a \frac{2z_1}{c}} + \gamma_{2L} \gamma_{2R} c_{ee} \left(t - \frac{2z_2}{c} \right) e^{i\omega_a \frac{2z_2}{c}}, \end{aligned} \quad (\text{A.13})$$

which is Eq. (9) in the main text.

Appendix B. Derivation of the interaction Hamiltonian in the spatial domain

When an atom is coupled with an infinite waveguide, the photonic wave packet can be divided into the right-propagating and left-propagating components. Accordingly, the Hamiltonian of the waveguide mode, given by the second term on the right-hand side of Eq. (1) in the main text, can be divided into two counter-propagating parts as (Bradford and Shen, 2013)

$$\int_0^\infty \omega_k d_k^\dagger d_k dk = \int_0^\infty \omega_{k_L} d_{k_L}^\dagger d_{k_L} dk_L + \int_0^\infty \omega_{k_R} d_{k_R}^\dagger d_{k_R} dk_R, \quad (\text{B.1})$$

where $d_{k_L}^\dagger$ (d_{k_L}) represents the creation (annihilation) operator of the left-moving photonic wave packet, and $d_{k_R}^\dagger$ (d_{k_R}) represents that of the right-moving photonic wave packet. Moreover, based on the linearization of the waveguide mode ω_k around a central frequency ω_0 , the left- and right-propagating modes can be represented as (Shen and Fan, 2009; Cyril Hewson, 1997)

$$\begin{cases} \int_0^\infty \omega_{k_L} d_{k_L}^\dagger d_{k_L} dk_L \simeq \int_0^\infty [\omega_0 - v_g(k_L - k_0)] d_{k_L}^\dagger d_{k_L} dk_L, \\ \int_0^\infty \omega_{k_R} d_{k_R}^\dagger d_{k_R} dk_R \simeq \int_0^\infty [\omega_0 + v_g(k_R - k_0)] d_{k_R}^\dagger d_{k_R} dk_R, \end{cases} \quad (\text{B.2})$$

where v_g is the group velocity of the field, $\omega_{k_L} \simeq \omega_0 - v_g(k_L - k_0)$ and $\omega_{k_R} \simeq \omega_0 + v_g(k_R - k_0)$. The creation and annihilation operators $d_{k_L}^\dagger$ and d_{k_L} for the left-propagating modes can be represented in terms of the spatial-domain operators as

$$\begin{cases} d_{k_L}^\dagger = \int_{-\infty}^\infty c_L^\dagger(z) e^{ik_L z} dz, \\ d_{k_L} = \int_{-\infty}^\infty c_L(z) e^{-ik_L z} dz, \end{cases} \quad (\text{B.3})$$

where $c_L^\dagger(z)$ and $c_L(z)$ are the creation and annihilation operators for the left-propagating field in the waveguide at position z , respectively. Similarly, for the right-propagating fields,

$$\begin{cases} d_{k_R}^\dagger = \int_{-\infty}^{\infty} c_R^\dagger(z) e^{ik_R z} dz, \\ d_{k_R} = \int_{-\infty}^{\infty} c_R(z) e^{-ik_R z} dz, \end{cases} \quad (\text{B.4})$$

with $c_R^\dagger(z)$ and $c_R(z)$ are the creation and annihilation operators for the right-propagating field in the waveguide at position z .

As for the chiral interaction part of the Hamiltonian, namely the right-hand side of Eq. (4) in the main text, the coupling is $g_{kl}(k, t, z)$ given in Eq. (5). Based on the transformation between the frequency domain and the spatial domain in Eqs. (B.3, B.4), the interaction Hamiltonian in the spatial domain is (Shen and Fan, 2009; Bradford and Shen, 2013)

$$H_I = -i \int_{-\infty}^{\infty} [\gamma_{1R} c_R(z) \delta(z - z_1) + \gamma_{1L} c_L(z) \delta(z - z_1)] \sigma_1^\dagger dz + \text{H.c.}, \quad (\text{B.5})$$

which gives the format of H_I in Eq. (43) in the main text. More details on the spatial modeling can be found in (Shen and Fan, 2009).

Appendix B.1. The Hamiltonian of the mirror

The function of the mirror in Fig. 1 is to reflect a left-moving photonic wave packet to a right-moving wave packet. Consider the circumstance that there are no atoms coupled with the waveguide. With the boundary of the mirror at $z = 0$, the Hamiltonian of the system in the absence of the atoms is

$$H' = H_w + H_m, \quad (\text{B.6})$$

where H_m represents the Hamiltonian of the mirror and H_w is the waveguide Hamiltonian given in Eq. (41). Let

$$|\Psi\rangle = \Theta(z) e^{ikz} c_R^\dagger(z) |0\rangle + \Theta(z) e^{-ikz} c_L^\dagger(z) |0\rangle, \quad (\text{B.7})$$

where Θ denotes the Heaviside step function.

Definition 1 (Bradford and Shen, 2013) *The quantum state $|\Psi\rangle$ in Eq. (B.7) is called an eigenstate corresponding to the eigen-spectrum $v_g k$ of the Hamiltonian H' if $H'|\Psi\rangle = v_g k |\Psi\rangle$.*

Lemma 4 *The Hamiltonian of the mirror located at the left terminal $z = 0$ is*

$$H_m = i2v_g \int_{0^-}^{\infty} [c_R^\dagger(z) c_L(z) e^{2ikz} - c_L^\dagger(z) c_R(z) e^{-2ikz}] \delta(z) dz. \quad (\text{B.8})$$

Proof The proof is constructive. For an eigenstate $|\Psi\rangle$ of the Hamiltonian $H' = H_m + H_w$, we have $(H_m + H_w)|\Psi\rangle = v_g k |\Psi\rangle$. Consequently,

$$\begin{aligned}
& (v_g k - H_w)|\Psi\rangle \\
&= \left(v_g k - iv_g \int_0^\infty dz c_L^\dagger(z) \frac{\partial}{\partial z} c_L(z) \right. \\
&+ \left. iv_g \int_0^\infty dz c_R^\dagger(z) \frac{\partial}{\partial z} c_R(z) \right) [\Theta(z) e^{ikz} c_R^\dagger(z)|0\rangle + \Theta(z) e^{-ikz} c_L^\dagger(z)|0\rangle] \\
&= v_g k |\Psi\rangle - iv_g \frac{\partial}{\partial z} [\Theta(z) e^{-ikz}] c_L^\dagger(z)|0\rangle + iv_g \frac{\partial}{\partial z} [\Theta(z) e^{ikz}] c_R^\dagger(z)|0\rangle \\
&= v_g k |\Psi\rangle - kv_g \Theta(z) e^{-ikz} c_L^\dagger(z)|0\rangle - kv_g \Theta(z) e^{ikz} c_R^\dagger(z)|0\rangle \\
&\quad - iv_g \delta(z) e^{-ikz} c_L^\dagger(z)|0\rangle + iv_g \delta(z) e^{ikz} c_R^\dagger(z)|0\rangle \\
&= v_g k |\Psi\rangle - kv_g |\Psi\rangle - iv_g \delta(z) e^{-ikz} c_L^\dagger(z)|0\rangle + iv_g \delta(z) e^{ikz} c_R^\dagger(z)|0\rangle \\
&= -iv_g \delta(z) e^{-ikz} c_L^\dagger(z)|0\rangle + iv_g \delta(z) e^{ikz} c_R^\dagger(z)|0\rangle.
\end{aligned} \tag{B.9}$$

On the other hand, for the form of H_m in Eq. (B.8), we have

$$\begin{aligned}
& H_m |\Psi\rangle \\
&= \int_{0^-}^\infty \left[i2v_g c_R^\dagger(z) c_L(z) e^{2ikz} \delta(z) - i2v_g c_L^\dagger(z) c_R(z) e^{-2ikz} \delta(z) \right] \\
&\quad dz \left[\Theta(z) e^{ikz} c_R^\dagger(z)|0\rangle + \Theta(z) e^{-ikz} c_L^\dagger(z)|0\rangle \right] \\
&= i2v_g \int_{0^-}^\infty \left[c_R^\dagger(z') c_L(z') e^{2ikz'} - c_L^\dagger(z') c_R(z') e^{-2ikz'} \right] \delta(z') dz' \\
&\quad \left[\Theta(z) e^{ikz} c_R^\dagger(z)|0\rangle + \Theta(z) e^{-ikz} c_L^\dagger(z)|0\rangle \right] \\
&= i2v_g \int_{0^-}^\infty c_R^\dagger(z') c_L(z') e^{2ikz'} \delta(z') dz' \Theta(z) e^{-ikz} c_L^\dagger(z)|0\rangle \\
&\quad - i2v_g \int_{0^-}^\infty c_L^\dagger(z') c_R(z') e^{-2ikz'} \delta(z') dz' \Theta(z) e^{ikz} c_R^\dagger(z)|0\rangle \\
&= i2v_g \int_{0^-}^\infty c_R^\dagger(z') e^{2ikz'} \delta(z') \delta(z - z') dz' \Theta(z) e^{-ikz} |0\rangle \\
&\quad - i2v_g \int_{0^-}^\infty c_L^\dagger(z') e^{-2ikz'} \delta(z') \delta(z - z') dz' \Theta(z) e^{ikz} |0\rangle \\
&= iv_g c_R^\dagger(z) \delta(z) \Theta(z) e^{ikz} |0\rangle - iv_g c_L^\dagger(z) \delta(z) \Theta(z) e^{-ikz} |0\rangle,
\end{aligned} \tag{B.10}$$

where the fact $\int_{0^-}^\infty \delta(z) \Theta(z) dz = 1/2$ has been used. As a result, when H_m is that in Eq. (B.9), $H'|\Psi\rangle = v_g k |\Psi\rangle$ holds.

□

Remark 10 The boundary condition of the waveguide given by the mirror is independent from whether the waveguide is coupled with the atom or not. The format of the Hamiltonian of the mirror is influenced by the relative position between the mirror and the waveguide. When the mirror is at the right terminal of the waveguide as adopted in (Bradford and Shen, 2013), the function of the mirror is to reflect the right-propagating fields in the waveguide to the

left-propagating fields, and the Hamiltonian of the mirror is different from the circumstance that the mirror is at the left terminal of the waveguide as given in Eq. (B.8) above.

Appendix C. One-atom model in the spatial domain

The quantum state with one right- or left propagating photon in the waveguide can be equivalently represented as in Eq. (42) and Eq. (45) in the main text, respectively. Substituting Eq. (45a) into Eq. (44b) yields

$$\begin{aligned}
& [\Theta(z) - \Theta(z - z_1)] \frac{\partial f_r(t - z/c)}{\partial t} + \Theta(z - z_1) \frac{\partial g_r(t - z/c)}{\partial t} \\
&= -v_g [\delta(z) - \delta(z - z_1)] f_r(t - z/c) - v_g [\Theta(z) - \Theta(z - z_1)] \frac{\partial f_r(t - z/c)}{\partial z} \\
&\quad - v_g \delta(z - z_1) g_r(t - z/c) - v_g \Theta(z - z_1) \frac{\partial g_r(t - z/c)}{\partial z} \\
&\quad + 2v_g \delta(z) [\Theta(z) - \Theta(z - z_1)] f_l(t + z/c) e^{2ikz} + \gamma_{1R} \delta(z - z_1) c_e(t) e^{-i\omega_a t}.
\end{aligned} \tag{C.1}$$

Noticing that $\frac{\partial f_r(t-z/c)}{\partial t} = -v_g \frac{\partial f_r(t-z/c)}{\partial z}$, and $\frac{\partial g_r(t-z/c)}{\partial t} = -v_g \frac{\partial g_r(t-z/c)}{\partial z}$, Eq. (C.1) reads

$$\begin{aligned}
& v_g [\delta(z) - \delta(z - z_1)] f_r(t - z/c) + v_g \delta(z - z_1) g_r(t - z/c) \\
&= 2v_g \delta(z) [\Theta(z) - \Theta(z - z_1)] f_l(t + z/c) e^{2ikz} + \gamma_{1R} \delta(z - z_1) c_e(t) e^{-i\omega_a t}.
\end{aligned} \tag{C.2}$$

Integrate both sides of Eq. (C.2) within $[z_1^-, z_1^+]$, we can derive that

$$-v_g f_r(t - z_1/c) + v_g g_r(t - z_1/c) = \gamma_{1R} c_e(t) e^{-i\omega_a t}. \tag{C.3}$$

For the left propagating mode, substituting Eq. (45b) into Eq. (44c) yields

$$\begin{aligned}
& [\Theta(z) - \Theta(z - z_1)] \frac{\partial f_l(t + z/c)}{\partial t} \\
&= v_g [\delta(z) - \delta(z - z_1)] f_l(t + z/c) + v_g [\Theta(z) - \Theta(z - z_1)] \frac{\partial f_l(t + z/c)}{\partial z} \\
&\quad + \gamma_{1L} \delta(z - z_1) c_e(t) e^{-i\omega_a t} - 2v_g \delta(z) \Phi_R(z, t) e^{-2ikz},
\end{aligned} \tag{C.4}$$

where $\frac{\partial f_l(t+z/c)}{\partial t} = v_g \frac{\partial f_l(t+z/c)}{\partial z}$, and hence Eq. (C.4) reads

$$\begin{aligned}
& 2v_g \delta(z) \Phi_R(z, t) e^{-2ikz} \\
&= v_g [\delta(z) - \delta(z - z_1)] f_l(t + z/c) + \gamma_{1L} \delta(z - z_1) c_e(t) e^{-i\omega_a t}.
\end{aligned} \tag{C.5}$$

From the integrals

$$\begin{aligned}
& \int_{z_1^-}^{z_1^+} 2v_g \delta(z) \Phi_R(z, t) e^{-2ikz} dz \\
&= \int_{z_1^-}^{z_1^+} v_g [\delta(z) - \delta(z - z_1)] f_l(t + z/c) dz + \int_{z_1^-}^{z_1^+} \gamma_{1L} \delta(z - z_1) c_e(t) e^{-i\omega_a t} dz,
\end{aligned} \tag{C.6}$$

and

$$\begin{aligned}
& \int_{0^-}^{0^+} 2v_g \delta(z) \Phi_R(z, t) e^{-2ikz} dz \\
&= \int_{0^-}^{0^+} v_g [\delta(z) - \delta(z - z_1)] f_i(t + z/c) dz \\
&+ \int_{0^-}^{0^+} \gamma_{1L} \delta(z - z_1) c_e(t) e^{-i\omega_a t} dz,
\end{aligned} \tag{C.7}$$

we have

$$\begin{cases} v_g f_i(t + z_1/c) = \gamma_{1L} c_e(t) e^{-i\omega_a t}, \\ 2v_g \Phi_R(0, t) = v_g f_i(t), \end{cases} \tag{C.8}$$

and

$$f_i(t) = \frac{\gamma_{1L}}{v_g} c_e(t - z_1/c) e^{-i\omega_a(t - z_1/c)}. \tag{C.9}$$

Combine Eqs. (C.3), (C.9) and (45) with the boundary condition $\Phi_R(0, t) = -\Phi_L(0, t)$ of the mirror at $z = 0$, we have

$$\begin{cases} -v_g f_r(t) + v_g g_r(t) = \gamma_{1R} c_e(t + z_1/c) e^{-i\omega_a(t + z_1/c)}, \\ f_i(t) = \frac{\gamma_{1L}}{v_g} c_e(t - z_1/c) e^{-i\omega_a(t - z_1/c)}, \\ f_i(t) = -f_r(t), \end{cases} \tag{C.10a}$$

$$f_i(t) = \frac{\gamma_{1L}}{v_g} c_e(t - z_1/c) e^{-i\omega_a(t - z_1/c)}, \tag{C.10b}$$

$$f_i(t) = -f_r(t), \tag{C.10c}$$

where the phase shift induced by the reflection of the mirror is omitted for the same reason as in Eq. (3) and Eq. (4) in the frequency domain analysis in the main text. Solving Eq. (C.10) we get

$$g_r(t) = \frac{\gamma_{1R}}{v_g} c_e(t + z_1/c) e^{-i\omega_a(t + z_1/c)} - \frac{\gamma_{1L}}{v_g} c_e(t - z_1/c) e^{-i\omega_a(t - z_1/c)}. \tag{C.11}$$

Considering that the amplitudes for the right and left propagating photons at $z = z_1$ can be represented as

$$\begin{cases} \Phi_R(z_1, t) = [\Theta(z_1) - \Theta(z_1 - z_1)] f_r(t - z_1/c) \\ \quad + \Theta(z_1 - z_1) g_r(t - z_1/c) \\ \quad = \frac{1}{2} f_r(t - z_1/c) + \frac{1}{2} g_r(t - z_1/c), \\ \Phi_L(z_1, t) = [\Theta(z_1) - \Theta(z_1 - z_1)] f_i(t + z_1/c) \\ \quad = \frac{1}{2} f_i(t + z_1/c), \end{cases} \tag{C.12}$$

where $\Theta(0) = 1/2$, and substitute $g_r(t)$, $f_l(t)$ and $f_r(t)$ obtained above into Eq. (44a), we get

$$\begin{aligned}
\dot{c}_e(t) &= -[\gamma_{1R}\Phi_R(z_1, t) + \gamma_{1L}\Phi_L(z_1, t)] e^{i\omega_a t} \\
&= -\frac{1}{2} [\gamma_{1R}(f_r(t - z_1/c) + g_r(t - z_1/c)) + \gamma_{1L}f_l(t + z_1/c)] e^{i\omega_a t} \\
&= -\frac{1}{2} \left\{ -\gamma_{1R} \frac{\gamma_{1L}}{v_g} c_e(t - 2z_1/c) e^{-i\omega_a(t-2z_1/c)} \right. \\
&\quad \left. + \gamma_{1R} \left[\frac{\gamma_{1R}}{v_g} c_e(t) e^{-i\omega_a t} - \frac{\gamma_{1L}}{v_g} c_e(t - 2z_1/c) e^{-i\omega_a(t-2z_1/c)} \right] \right. \\
&\quad \left. + \gamma_{1L} \frac{\gamma_{1L}}{v_g} c_e(t) e^{-i\omega_a t} \right\} e^{i\omega_a t} \\
&= -\frac{\gamma_{1R}^2 + \gamma_{1L}^2}{2v_g} c_e(t) + \frac{\gamma_{1L}\gamma_{1R}}{v_g} c_e(t - 2z_1/c) e^{i2\omega_a z_1/c},
\end{aligned} \tag{C.13}$$

which is Eq. (46) in the main text.

Appendix D. Two-atom model with one excitation in the spatial domain

Substituting the state representation in Eq. (57) into Eq. (56) in the main text, we have

$$\begin{cases} v_g [\delta(z) - \delta(z - z_1)] f_r(t - z/c) + v_g \delta(z - z_2) h_r(t - z/c) \\ + v_g [\delta(z - z_1) - \delta(z - z_2)] g_r(t - z/c) \\ = 2v_g \Phi_g^l(t, z) e^{2ikz} \delta(z) + \sum_{j=1,2} \gamma_{jR} c_j(t) \delta(z - z_j) e^{-i\omega_a t}, \end{cases} \tag{D.1a}$$

$$\begin{cases} v_g [\delta(z) - \delta(z - z_1)] f_l(t + z/c) + v_g [\delta(z - z_1) - \delta(z - z_2)] g_l(t + z/c) \\ = 2v_g \delta(z) \Phi_g^r(t, z) e^{-2ikz} \delta(z) - \sum_{j=1,2} \gamma_{jL} c_j(t) \delta(z - z_j) e^{-i\omega_a t}. \end{cases} \tag{D.1b}$$

Consider the integration within $[0^-, 0^+]$, $[z_1^-, z_1^+]$ and $[z_2^-, z_2^+]$ respectively, we have

$$f_r(t) = -f_l(t), \tag{D.2a}$$

$$g_r(t - z_1/c) - f_r(t - z_1/c) = \frac{\gamma_{1R}}{v_g} c_1(t) e^{-i\omega_a t}, \tag{D.2b}$$

$$g_l(t + z_1/c) - f_l(t + z_1/c) = -\frac{\gamma_{1L}}{v_g} c_1(t) e^{-i\omega_a t}, \tag{D.2c}$$

$$h_r(t - z_2/c) - g_r(t - z_2/c) = \frac{\gamma_{2R}}{v_g} c_2(t) e^{-i\omega_a t}, \tag{D.2d}$$

$$g_l(t + z_2/c) = \frac{\gamma_{2L}}{v_g} c_2(t) e^{-i\omega_a t}. \tag{D.2e}$$

Then

$$\begin{aligned}
\dot{c}_1(t) &= -\gamma_{1R}\Phi_g^r(t, z_1)e^{i\omega_a t} - \gamma_{1L}\Phi_g^l(t, z_1)e^{i\omega_a t} \\
&= -\gamma_{1R}\frac{f_r(t - z_1/c) + g_r(t - z_1/c)}{2}e^{i\omega_a t} - \gamma_{1L}\frac{f_l(t + z_1/c) + g_l(t + z_1/c)}{2}e^{i\omega_a t} \\
&= \frac{\gamma_{1R}^2 + \gamma_{1L}^2}{2}c_1(t) - \gamma_{1R}g_r(t - z_1/c)e^{i\omega_a t} - \gamma_{1L}f_l(t + z_1/c)e^{i\omega_a t} \\
&= -\frac{\gamma_{1R}^2 + \gamma_{1L}^2}{2}c_1(t) + \gamma_{1R}\gamma_{1L}c_1\left(t - \frac{2z_1}{c}\right)e^{i\omega_a \frac{2z_1}{c}} \\
&\quad + \gamma_{1R}\gamma_{2L}c_2\left(t - \frac{z_1 + z_2}{c}\right)e^{i\omega_a \frac{z_1 + z_2}{c}} - \gamma_{1L}\gamma_{2L}c_2\left(t - \frac{z_2 - z_1}{c}\right)e^{i\omega_a \frac{z_2 - z_1}{c}},
\end{aligned} \tag{D.3}$$

$$\begin{aligned}
g_r(t - z_1/c) &= f_r(t - z_1/c) + \frac{\gamma_{1R}}{v_g}c_1(t)e^{-i\omega_a t} \\
&= f_l(t - z_1/c) + \frac{\gamma_{1R}}{v_g}c_1(t)e^{-i\omega_a t} \\
&= g_l(t - z_1/c) + \frac{\gamma_{1L}}{v_g}c_1\left(t - \frac{2z_1}{c}\right)e^{-i\omega_a(t - \frac{2z_1}{c})} + \frac{\gamma_{1R}}{v_g}c_1(t)e^{-i\omega_a t} \\
&= \frac{\gamma_{2L}}{v_g}c_2\left(t - \frac{z_1 + z_2}{c}\right)e^{-i\omega_a(t - \frac{z_1 + z_2}{c})} + \frac{\gamma_{1L}}{v_g}c_1\left(t - \frac{2z_1}{c}\right)e^{-i\omega_a(t - \frac{2z_1}{c})} + \frac{\gamma_{1R}}{v_g}c_1(t)e^{-i\omega_a t},
\end{aligned} \tag{D.4}$$

and

$$\begin{aligned}
f_l(t + z_1/c) &= g_l(t + z_1/c) + \frac{\gamma_{1L}}{v_g}c_1(t)e^{-i\omega_a t} \\
&= \frac{\gamma_{2L}}{v_g}c_2\left(t - \frac{z_2 - z_1}{c}\right)e^{-i\omega_a(t - \frac{z_2 - z_1}{c})} + \frac{\gamma_{1L}}{v_g}c_1(t)e^{-i\omega_a t}.
\end{aligned} \tag{D.5}$$

Similarly,

$$\begin{aligned}
\dot{c}_2(t) &= -\frac{\gamma_{2R}^2 + \gamma_{2L}^2}{2}c_2(t) + \gamma_{2R}\gamma_{2L}c_2\left(t - \frac{2z_2}{c}\right)e^{i\omega_a \frac{2z_2}{c}} \\
&\quad + \gamma_{1L}\gamma_{2R}c_1\left(t - \frac{z_1 + z_2}{c}\right)e^{i\omega_a \frac{z_1 + z_2}{c}} - \gamma_{1R}\gamma_{2R}c_1\left(t - \frac{z_2 - z_1}{c}\right)e^{i\omega_a \frac{z_2 - z_1}{c}}.
\end{aligned} \tag{D.6}$$

By Eq. (D.2), the photonic wave packet in the spatial domain is

$$\left\{ \begin{aligned} g_l(t + z/c) &= \frac{\gamma_{2L}}{v_g}c_2(t + z/c - z_2/c)e^{-i\omega_a(t + z/c - z_2/c)}, \end{aligned} \right. \tag{D.7a}$$

$$\left\{ \begin{aligned} f_l(t + z/c) &= \frac{\gamma_{2L}}{v_g}c_2(t + z/c - z_2/c)e^{-i\omega_a(t + z/c - z_2/c)} \\ &\quad + \frac{\gamma_{1L}}{v_g}c_1(t + z/c - z_1/c)e^{-i\omega_a(t + z/c - z_1/c)}, \end{aligned} \right. \tag{D.7b}$$

$$\left\{ \begin{aligned} f_r(t - z/c) &= -\frac{\gamma_{2L}}{v_g}c_2(t - z/c - z_2/c)e^{-i\omega_a(t - z/c - z_2/c)} \\ &\quad - \frac{\gamma_{1L}}{v_g}c_1(t - z/c - z_1/c)e^{-i\omega_a(t - z/c - z_1/c)}, \end{aligned} \right. \tag{D.7c}$$

$$\left\{ \begin{aligned} g_r(t - z/c) &= f_r(t - z/c) \\ &\quad + \frac{\gamma_{1R}}{v_g}c_1(t - z/c + z_1/c)e^{-i\omega_a(t - z/c + z_1/c)}, \end{aligned} \right. \tag{D.7d}$$

$$\left\{ \begin{aligned} h_r(t - z/c) &= g_r(t - z/c) \\ &\quad + \frac{\gamma_{2R}}{v_g}c_2(t - z/c + z_2/c)e^{-i\omega_a(t - z/c + z_2/c)}. \end{aligned} \right. \tag{D.7e}$$

Acknowledgement

GFZ acknowledges supports from Innovation Program for Quantum Science, Technology 2023ZD0300600, Guangdong Provincial Quantum Science Strategic Initiative (No. GDZX2200001), the Hong Kong Research Grant council (RGC) Grants No. 15213924, and the CAS AMSS-PolyU Joint Laboratory of Applied Mathematics. MTC and GQC acknowledge supports by National Nature Science Foundation of China with grant Nos.119075023, 12475010, and Key Project of Natural Science Foundation of Anhui Provincial Department of Education under Grant 2022AH040053.

References

- Almendros, M., Huwer, J., Piro, N., Rohde, F., Schuck, C., Hennrich, M., Dubin, F., Eschner, J., 2009. Bandwidth-tunable single-photon source in an ion-trap quantum network. *Physical Review Letters* 103, 213601.
- Angulo, S., Márquez, R., Bernal, M., 2019. Quasi-polynomial-based robust stability of time-delay systems can be less conservative than Lyapunov–Krasovskii approaches. *IEEE Transactions on Automatic Control* 65, 3164–3169.
- Barros, H., Stute, A., Northup, T., Russo, C., Schmidt, P., Blatt, R., 2009. Deterministic single-photon source from a single ion. *New Journal of Physics* 11, 103004.
- Bradford, M., Shen, J.T., 2013. Spontaneous emission in cavity QED with a terminated waveguide. *Physical Review A* 87, 063830.
- Bradford, M., Shen, J.T., 2015. Architecture dependence of photon antibunching in cavity quantum electrodynamics. *Physical Review A* 92, 023810.
- Busse, G., Reinert, J., Jacob, A.F., 1999. Waveguide characterization of chiral material: Experiments. *IEEE Transactions on Microwave Theory and Techniques* 47, 297–301.
- Cardona, G., Sarlette, A., Rouchon, P., 2020. Exponential stabilization of quantum systems under continuous non-demolition measurements. *Automatica* 112, 108719.
- Chen, Z., Zhou, Y., Shen, J.T., 2017. Dissipation-induced photonic-correlation transition in waveguide-QED systems. *Physical Review A* 96, 053805.
- Cheng, M.T., Xu, J., Agarwal, G.S., 2017. Waveguide transport mediated by strong coupling with atoms. *Physical Review A* 95, 053807.
- Crowder, G., Carmichael, H., Hughes, S., 2020. Quantum trajectory theory of few-photon cavity-QED systems with a time-delayed coherent feedback. *Physical Review A* 101, 023807.
- Cyril Hewson, A., 1997. *The Kondo Problem to Heavy Fermions*.
- Dinc, F., 2020. Diagrammatic approach for analytical non-Markovian time evolution: Fermi’s two-atom problem and causality in waveguide quantum electrodynamics. *Physical Review A* 102, 013727.
- Ding, H., Amini, N.H., Zhang, G., Gough, J.E., 2023. Quantum coherent and measurement feedback control based on atoms coupled with a semi-infinite waveguide. *arXiv preprint arXiv:2307.16876*.
- Ding, H., Zhang, G., 2023. Quantum coherent feedback control with photons. *IEEE Transactions on Automatic Control* 69, 856–871.
- Domokos, P., Horak, P., Ritsch, H., 2002. Quantum description of light-pulse scattering on a single atom in waveguides. *Physical Review A* 65, 033832.
- Dorner, U., Zoller, P., 2002. Laser-driven atoms in half-cavities. *Physical Review A* 66, 023816.
- Flamini, F., Spagnolo, N., Sciarrino, F., 2018. Photonic quantum information processing: a review. *Reports on Progress in Physics* 82, 016001.
- Gea-Banacloche, J., 2013. Space-time descriptions of quantum fields interacting with optical cavities. *Physical Review A—Atomic, Molecular, and Optical Physics* 87, 023832.
- Gea-Banacloche, J., Lu, N., Pedrotti, L.M., Prasad, S., Scully, M.O., Wódkiewicz, K., 1990. Treatment of the spectrum of squeezing based on the modes of the universe. I. Theory and a physical picture. *Physical Review A* 41, 369.

- Gonzalez-Ballesterro, C., Gonzalez-Tudela, A., Garcia-Vidal, F.J., Moreno, E., 2015. Chiral route to spontaneous entanglement generation. *Physical Review B* 92, 155304.
- Guimond, P.O., Pletyukhov, M., Pichler, H., Zoller, P., 2017. Delayed coherent quantum feedback from a scattering theory and a matrix product state perspective. *Quantum Science and Technology* 2, 044012.
- Hijlkema, M., Weber, B., Specht, H.P., Webster, S.C., Kuhn, A., Rempe, G., 2007. A single-photon server with just one atom. *Nature Physics* 3, 253–255.
- Houck, A.A., Schuster, D., Gambetta, J., Schreier, J., Johnson, B., Chow, J., Frunzio, L., Majer, J., Devoret, M., Girvin, S., et al., 2007. Generating single microwave photons in a circuit. *Nature* 449, 328–331.
- Hu, Q., Zou, B., Zhang, Y., 2018. Transmission and correlation of a two-photon pulse in a one-dimensional waveguide coupled with quantum emitters. *Physical Review A* 97, 033847.
- Huo, M., Li, Y., 2020. Absorption and delayed reemission in an array of atoms strongly coupled to a waveguide. *Physical Review A* 102, 033728.
- Kamen, E., 1980. On the relationship between zero criteria for two-variable polynomials and asymptotic stability of delay differential equations. *IEEE Transactions on Automatic Control* 25, 983–984.
- Kamen, E., 1982. Linear systems with commensurate time delays: Stability and stabilization independent of delay. *IEEE Transactions on Automatic Control* 27, 367–375.
- Kashima, K., Yamamoto, N., 2009. Control of quantum systems despite feedback delay. *IEEE Transactions on Automatic Control* 54, 876–881.
- Keller, M., Lange, B., Hayasaka, K., Lange, W., Walther, H., 2004. Continuous generation of single photons with controlled waveform in an ion-trap cavity system. *Nature* 431, 1075–1078.
- Kockum, A.F., Johansson, G., Nori, F., 2018. Decoherence-free interaction between giant atoms in waveguide quantum electrodynamics. *Physical Review Letters* 120, 140404.
- Kuhn, A., Hennrich, M., Rempe, G., 2002. Deterministic single-photon source for distributed quantum networking. *Physical Review Letters* 89, 067901.
- La, R.J., Ranjan, P., 2007. Asymptotic stability of a rate control system with communication delays. *IEEE Transactions on Automatic Control* 52, 1920–1925.
- Laakso, M., Pletyukhov, M., 2014. Scattering of two photons from two distant qubits: Exact solution. *Physical Review Letters* 113, 183601.
- Lang, R., Scully, M.O., Lamb Jr, W.E., 1973. Why is the laser line so narrow? a theory of single-quasimode laser operation. *Physical Review A* 7, 1788.
- Li, X., Song, S., 2016. Stabilization of delay systems: delay-dependent impulsive control. *IEEE Transactions on Automatic Control* 62, 406–411.
- Lodahl, P., Mahmoodian, S., Stobbe, S., Rauschenbeutel, A., Schneeweiss, P., Volz, J., Pichler, H., Zoller, P., 2017. Chiral quantum optics. *Nature* 541, 473–480.
- Mariotte, F., Engheta, N., 1993. Reflection and transmission of guided electromagnetic waves at an air-chiral interface and at a chiral slab in a parallel-plate waveguide. *IEEE Transactions on Microwave Theory and Techniques* 41, 1895–1906.
- Michler, P., Kiraz, A., Becher, C., Schoenfeld, W., Petroff, P., Zhang, L., Hu, E., Imamoglu, A., 2000. A quantum dot single-photon turnstile device. *Science* 290, 2282–2285.
- Mirza, I.M., Schotland, J.C., 2016. Two-photon entanglement in multiqubit bidirectional-waveguide QED. *Physical Review A* 94, 012309.
- Monroe, C., 2002. Quantum information processing with atoms and photons. *Nature* 416, 238–246.
- Német, N., Carmele, A., Parkins, S., Knorr, A., 2019. Comparison between continuous- and discrete-mode coherent feedback for the Jaynes-Cummings model. *Physical Review A* 100, 023805.
- Northup, T., Blatt, R., 2014. Quantum information transfer using photons. *Nature Photonics* 8, 356–363.
- Olbrot, A., 1984. A sufficiently large time delay in feedback loop must destroy exponential stability of any decay rate. *IEEE Transactions on Automatic Control* 29, 367–368.
- Peng, Z., De Graaf, S., Tsai, J., Astafiev, O., 2016. Tuneable on-demand single-photon source in the microwave range. *Nature Communications* 7, 1–6.

- Pichler, H., Zoller, P., 2016. Photonic circuits with time delays and quantum feedback. *Physical Review Letters* 116, 093601.
- Qiao, L., Sun, C.P., 2019. Atom-photon bound states and non-Markovian cooperative dynamics in coupled-resonator waveguides. *Physical Review A* 100, 063806.
- Regidor, S.A., Crowder, G., Carmichael, H., Hughes, S., 2021. Modeling quantum light-matter interactions in waveguide QED with retardation, nonlinear interactions, and a time-delayed feedback: Matrix product states versus a space-discretized waveguide model. *Physical Review Research* 3, 023030.
- Shen, J.T., Fan, S., 2009. Theory of single-photon transport in a single-mode waveguide. I. Coupling to a cavity containing a two-level atom. *Physical Review A* 79, 023837.
- Simon, C., 2017. Towards a global quantum network. *Nature Photonics* 11, 678–680.
- Sinha, K., González-Tudela, A., Lu, Y., Solano, P., 2020. Collective radiation from distant emitters. *Physical Review A* 102, 043718.
- Söllner, I., Mahmoodian, S., Hansen, S.L., Midolo, L., Javadi, A., Kiršanskė, G., Pregolato, T., El-Ella, H., Lee, E.H., Song, J.D., et al., 2015. Deterministic photon-emitter coupling in chiral photonic circuits. *Nature Nanotechnology* 10, 775–778.
- Soro, A., Kockum, A.F., 2022. Chiral quantum optics with giant atoms. *Physical Review A* 105, 023712.
- Tan, H.T., Zhang, W.M., Li, G.x., 2011. Entangling two distant nanocavities via a waveguide. *Physical Review A* 83, 062310.
- Tao, B., Xiao, M., Zheng, W.X., Zhou, Y., Ding, J., Jiang, G., Wu, X., 2022. Design and dynamics analysis of a time-delay feedback controller with distributed characteristic. *IEEE Transactions on Automatic Control* 68, 1926–1933.
- Tufarelli, T., Ciccarello, F., Kim, M.S., 2013. Dynamics of spontaneous emission in a single-end photonic waveguide. *Physical Review A* 87, 013820.
- Yamamoto, N., 2014. Coherent versus measurement feedback: Linear systems theory for quantum information. *Physical Review X* 4, 041029.
- Yan, C.H., Wei, L.F., Jia, W.Z., Shen, J.T., 2011. Controlling resonant photonic transport along optical waveguides by two-level atoms. *Physical Review A* 84, 045801.
- Zhang, B., You, S., Lu, M., 2020. Enhancement of spontaneous entanglement generation via coherent quantum feedback. *Physical Review A* 101, 032335.
- Zhang, G., 2020. Single-photon coherent feedback control and filtering. *Encyclopedia of Systems and Control*. Springer, London .
- Zhang, G., Dong, Z., 2022. Linear quantum systems: a tutorial. *Annual Reviews in Control* 54, 274–294.
- Zhang, G., James, M.R., 2010. Direct and indirect couplings in coherent feedback control of linear quantum systems. *IEEE Transactions on Automatic Control* 56, 1535–1550.
- Zhang, G., Pan, Y., 2020. On the dynamics of two photons interacting with a two-qubit coherent feedback network. *Automatica* 117, 108978.
- Zhang, J., Liu, Y.X., Wu, R.B., Jacobs, K., Nori, F., 2017. Quantum feedback: Theory, experiments, and applications. *Physics Reports* .
- Zheng, H., Baranger, H.U., 2013. Persistent quantum beats and long-distance entanglement from waveguide-mediated interactions. *Physical Review Letters* 110, 113601.
- Zhou, Y., Chen, Z., Shen, J.T., 2017. Single-photon superradiant emission rate scaling for atoms trapped in a photonic waveguide. *Physical Review A* 95, 043832.
- Zwiller, V., Blom, H., Jonsson, P., Panev, N., Jeppesen, S., Tsegaye, T., Goobar, E., Pistol, M.E., Samuelson, L., Björk, G., 2001. Single quantum dots emit single photons at a time: Antibunching experiments. *Applied Physics Letters* 78, 2476–2478.